A "Four Core Genotypes" rat model to distinguish mechanisms underlying sex-biased phenotypes and diseases

Arthur P. Arnold[1], Xuqi Chen[1], Michael N. Grzybowski[2], Janelle M. Ryan[3], Dale R. Sengelaub[4], Tara Mohanroy[1], V. Andree Furlan[1], William Grisham[5], Lynn Malloy[2], Akiko Takizawa[2], Carrie B. Wiese[6], Laurent Vergnes[6], Helen Skaletsky[7], David C. Page[7], Karen Reue[6], Vincent R. Harley[3], Melinda R. Dwinell[2], and Aron M. Geurts[2]

[1] Department of Integrative Biology & Physiology, and Laboratory of Neuroendocrinology of the Brain Research Institute, University of California, Los Angeles, Los Angeles 90095 CA USA

[2] Department of Physiology, Medical College of Wisconsin, Milwaukee, WI 53226, USA.

[3] Hudson Institute of Medical Research, Monash Medical Centre, Melbourne, Australia.

[4] Department of Psychological and Brain Sciences, Indiana University, Bloomington, IN, USA

[5] Department of Psychology, University of California, Los Angeles, Los Angeles, CA 90095, USA

[6] Department of Human Genetics, David Geffen School of Medicine at UCLA, Los Angeles, 90095 CA, USA

[7] Howard Hughes Medical Institute, Whitehead Institute, Cambridge MA, USA

Abstract

Background

We have generated a rat model similar to the Four Core Genotypes mouse model, allowing comparison of XX and XY rats with the same type of gonad. The model detects novel sex chromosome effects (XX vs. XY) that contribute to sex differences in any rat phenotype.

Methods

XY rats were produced with an autosomal transgene of *Sry*, the testis-determining factor gene, which were fathers of XX and XY progeny with testes. In other rats, CRISPR-Cas9 technology was used to remove Y chromosome factors that initiate testis differentiation, producing fertile XY gonadal females that have XX and XY progeny with ovaries. These groups can be compared to detect sex differences caused by sex chromosome complement (XX vs. XY) and/or by gonadal hormones (rats with testes vs. ovaries).

Results

We have measured numerous phenotypes to characterize this model, including gonadal histology, breeding performance, anogenital distance, levels of reproductive hormones, body and organ weights, and central nervous system sexual dimorphisms. Serum testosterone levels were comparable in adult XX and XY gonadal males. Numerous phenotypes previously found to be sexually differentiated by the action of gonadal hormones were found to be similar in XX and XY rats with the same type of gonad, suggesting that XX and XY rats with the same type of gonad have comparable levels of gonadal hormones at various stages of development.

Conclusion

The results establish a powerful new model to discriminate sex chromosome and gonadal hormone effects that cause sexual differences in rat physiology and disease.

Introduction

Biological sex differences in physiology and disease are caused by two main classes of sex-biased factors, gonadal hormones (ovarian vs. testicular), and sex chromosome complement (XX vs. XY) [1]. Distinguishing the effects of sex chromosome complement has been challenging, because the sex chromosomal and hormonal factors are normally tightly linked in comparisons of wild-type XX gonadal females and XY gonadal males. The Four Core Genotypes (FCG) mouse model has been useful in separating these effects, by unlinking sex chromosome complement from differentiation of gonads [2-4]. In FCG mice, the testis-determining gene *Sry* is deleted from the Y chromosome (ChrY), producing a variant ChrY ("Y⁻") that does not regulate gonadal type [5]. The insertion of a functional *Sry* transgene into an autosome complements the loss of *Sry*, so that XY⁻(*Sry*TG+) mice have testes and are fertile [6, 7]. They produce four types of offspring: XX and XY mice with the *Sry* transgene and testes, and XX and XY mice lacking *Sry* and possessing ovaries. In this model, sex chromosome effects on phenotypes are measured by comparing XX and XY mice with the same type of gonad (either testes or ovaries), and hormone effects on any phenotype are measured by comparing mice with different types of gonads but with the same type of sex chromosomes (either XX or XY). Use of FCG mice has led to the novel discovery of sex chromosome effects that contribute to sex differences in body weight and adiposity, autoimmune disease, Alzheimer's disease, numerous cardiovascular diseases, neural tube closure defects, and the brain and behavior [8-16]. Use of FCG mice confirmed gonadal hormonal control of other sex differences [2, 14, 17, 18]

A significant limitation is that the FCG model has only been available in mice. It is important to avoid an overreliance on a single species as the only animal model system in which important biomedical questions can be addressed. Any fundamental question of biology (such as sex-biasing effects of sex chromosomes in non-gonadal tissues) must be studied in diverse species to achieve a general answer. Here we report the development of an FCG model in laboratory rats (*Rattus norvegicus*) as a second species in which sex chromosome effects can be studied with relative ease. Rats have many advantages as a model species because of the vast literature on rat sex differences, their greater utility in some models of human disease, and their larger size [19-22]. Transgenesis is used increasingly in rats, and rat genomic and epigenomic resources are being rapidly developed [23-28].

We produced a rat FCG model by following the approach used to make FCG mice. We generated a rat ChrY that does not cause formation of testes, and inserted a functional *Sry* transgene into an autosome. A significant complication is that rats possess 8-11 different *Sry* genes on ChrY, depending on strain [29]. The *Sry* gene(s) causing differentiation of testes, as individual genes or in combination, are not known. We previously reported that at least three *Sry* genes (*Sry4a*, *Sry1*, and *Sry3c*) are expressed in the gonadal ridge as it begins testis differentiation at embryonic day 13 (21 tail somites) in Sprague Dawley rats [30]. Therefore as a transgene, we used a single Bacterial Artificial Chromosome (BAC) clone encoding all three of these *Sry* genes and no other genes. We report here the production of XY gonadal males with an autosomal *Sry* BAC transgene that causes testis development in XX offspring, allowing comparison of XX and XY gonadal males. To interfere with the testis-determining function of ChrY, we utilized CRISPR gRNAs aimed at ChrY regions near *Sry4a* and *Sry1*. This method produced fertile XY gonadal females that had XX and XY offspring with ovaries. Together, these resources provide an avenue for investigating sex chromosome effects in virtually any rat phenotype. We report here the development of these resources and initial investigations of phenotypes.

Methods

All experiments were approved by the Institutional Animal Care and Use Committees of participating institutions. Here, "male" and "female" are defined by type of gonad.

Production of XX(SryTG+) gonadal male rats

Based on our previous evidence for expression of *Sry4a, Sry3C,* and *Sry1* in the embryonic gonadal ridge at the onset of rat testis development [30], we selected a single BAC clone RNECO-180E22 (Genbank AC279199) encoding these genes and no other known genes. At the Medical College of Wisconsin (MCW), we demonstrated by pronuclear microinjection into zygotes that a transgene, comprising this BAC clone and the pCC1BAC plasmid vector, caused formation of testes in a single transgenic XX female founder rat. Because XX gonadal males lack sperm, the model could not be propagated. At the University of Michigan Animal Model

Core, this BAC was purified and injected into pronuclei of more Sprague Dawley CD zygotes (Charles River Laboratories, Crl:CD(SD) strain code 001) to generate 22 founder rats carrying the transgene. Of 22 founders, 11 were XX, of which 6 were gonadal males. Four lines of XY transgenic founders [CD-Tg(RNECO-180E22)208Arno (RGD:155663365), CD-Tg(RNECO-180E22)733Arno (RGD:155663367), CD-Tg(RNECO-180E22)424Arno (RGD:155663366), and CD-Tg(RNECO-180E22)737Arno (RGD:155663368)] transmitted the transgene to XX offspring that were gonadal males. Hereafter we will simply refer to the line numbers 208, 733, 424, and 737. We backcrossed all four transgenic lines to the Sprague Dawley Crl:CD(SD) strain (Charles River, Wilmington MA) for at least 10 generations to isolate a single transgene integration site in each line, and to measure phenotypes. Mating XXWT females to XY(*Sry*TG+) males produced XXWT gonadal females, and three types of gonadal males: XYWT, XX(*Sry*TG+) and XY(*Sry*TG+) (Figure 1, Table 1, hereafter called XYWT, XXTG and XYTG, respectively). Offspring genotype was determined by PCR as discussed below.

Production and genomic characterization of XY$^{\Delta}$ gonadal female rats

The same BAC clone RNECO-180E22 sequence was used to design SpyCas9 guide RNAs flanking ~67 kilobases of ChrY sequence harboring *Sry4a* and *Sry1* where unique sites could be identified in an attempt to delete both genes. XY$^{\Delta}$ mutant rats [SD-Del(Yp)1Mcwi (RGD:155663364)] were generated at MCW by pronuclear injection of these two CRISPR-Cas9 ribonucleoproteins targeting the sequences GCATGTGGGCAGTTTCCACC<u>TGG</u> and ACACAGCTCCTCTCTGGTAG<u>AGG</u> (protospacer adjacent motif underlined) into single-cell Crl:SD (Charles River Laboratories, Crl:SD strain code 400) embryos. A single gonadal female carrying ChrY was identified. This female was fertile and successfully transmitted the mutant ChrY following backcross to a wild-type XY Crl:SD male. Mating XY$^{\Delta}$ females to XYWT males produced litters with XYWT males, XXWT females, and XY$^{\Delta}$ females (Figure 1, Table 1). XY$^{\Delta}$ females were backcrossed to Crl:CD(SD) XYWT males for up to 7 generations. To provide a preliminary analysis of the CRISPR-induced genomic lesion in this model, genomic DNA was harvested from spleen of an individual XY$^{\Delta}$ mutant rat and a control Crl:SD male rat and prepared for Illumina 150-bp paired-end whole genome sequencing (WGS) by the MCW Mellowes Center for Genomic Sciences and Precision Medicine on the Novaseq S4 flow cell to generate 30X coverage. Quality filtered reads were mapped to a modified Brown Norway (BN) rat reference genome mRatBN7.2 (rn7, [31]) where the reference ChrY and unmapped ChrY contigs were removed and replaced with an assembly of ~1.8-Mbp of Yp from the Spontaneously Hypertensive Rat (SHR) strain (GeneBank accession: OP905629).

Genotyping

Offspring genotype was determined by PCR. DNA was extracted from tails by using Chelex resin (Bio-Rad Laboratories, Hercules, CA). Presence of ChrY was detected using primers that amplify *Med14X* and *Med14Y* (forward primer CCTCCAGACCCTATTACCAA, reverse primer ATCACTGTCAAGGTTGCTTC) producing a 560 bp product for *Med14X* and a 172 bp product for *Med14Y*. Presence of the *Sry* BAC transgene was determined using primers spanning each end of the 180E22 BAC clone and the adjacent pCC1BAC vector sequence (180E22.1 forward primer GCAAAGGTTATGACAGGGAAA, and reverse primer CCTCTTCGCTATTACGCCAG with expected PCR product 259bp, and 180E22.2 forward primer: TGTGGAATTGTGAGCGGATA, and reverse primer: TCTGCTGTCCCCTGAGTTTT with expected PCR product 294bp). The Y$^{\Delta}$ chromosome was detected by using forward primer GCTGGGATGGGAAACAGGCTAC and reverse primer GAGCTAGGTAGGGACAGGAGTGGG with expected PCR product of 218 bp compared to 239bp from intact ChrY.

Gonadal histology

Testes and ovaries were dissected out from rats at approximately postnatal day 60 (~P60, P1 is the day of birth) and immersed in freshly prepared 4% paraformaldehyde (PFA) overnight at 4°C. They were transferred to 70% alcohol before embedding in paraffin for later sectioning. The gonads were sectioned at 4µm and sections collected on Superfrost slides. Hematoxylin and Eosin staining was performed by the Monash Histology Facility using established protocols [32]. Stained slides were imaged using the Leica Aperio VS120 Microscope and processed using the Leica ImageScope software.

Sry expression in tissues

Spleen, liver, and gonads were dissected out from P60-65 male rats from lines 208 and 733 at backcross generation 7, and from XX and XY^{Δ} female rats at backcross generation 4. They were flash frozen in liquid nitrogen, then stored at −80°C until further use. RNA was isolated from tissues with Trizol (Invitrogen, Carlsbad, CA, USA) and treated with ezDNase (Invitrogen) to prevent possible contamination with genomic DNA. First-strand cDNA was generated using cDNA reverse transcription kit (Applied Biosystems, Foster City, CA, USA) using oligo dT12-18 primers (Invitrogen) instead of random primers. Quantitative real time PCR (n=7–8 per genotype) was performed on an ABI 7300 Sequence Detection system (Applied Biosystems) using the PowerUp SYBR Green Master Mix Kit (Applied Biosystems).

Pan-*Sry* primers (forward TTGCAGCGTGAAGTTGCCTC and reverse TCTGGTTCTTGGAGGACTGG) were used to amplify all the *Sry* genes except the *nonHMGSry* gene. TATA box-binding protein (TBP: forward GTGAAGGGTACAAGGGGGTG, reverse ACATCTCAGCAACCCACACA) and 36B4 (forward GCCAGGCGTCCTCATTAGA, reverse CATCTGCTTGGAGCCCACA) were used as loading control genes. Cycling conditions were: 95°C for 3 min; 40 cycles of 95°C for 15 sec, 60°C for 30 sec and 72°C for 30 sec. with standard curve for *Sry* gene and control genes with four serial dilution points of control cDNA. Dissociation curves were applied to eliminate the possibility of genomic DNA contamination. Expression of *Sry* was expressed as fold change relative to the control gene.

Growth curves and organ weights

Rats were group-housed and maintained at 23°C on a 12:12 light/dark cycle. Rats were fed regular chow diet with 5% fat (LabDiet 5001, St. Louis, MO, USA). Body weight was measured at P21 and then at weekly intervals until ~P60, at background generation 7. At ~P60, spleens, kidneys and gonads were dissected and weighed.

Three depots of white adipose tissue (inguinal, gonadal, retroperitoneal) were dissected from P85-91 XYWT, XXTG, and XYTG males of backcross generation 1 of line 208, and from XXWT and XY^{Δ} females in backcross generation 1. The weight of each depot was expressed as a percentage of body weight.

Anogenital distance

Anogenital distance (AGD) was measured at P6-7 at backcross generation 7 for transgenic litters, and generation 2 for knockout litters. Because of variability in body size across litters, each rat's absolute AGD was expressed as a ratio relative to the mean AGD of XY rats in its litter.

S***erum testosterone, follicle-stimulating hormone (FSH) and luteinizing hormone (LH) levels***

Whole blood was collected using cardiac puncture from isoflurane-anesthetized rats at ~P60. Blood was allowed to clot at room temperature for more than 60 minutes, and then centrifuged at 1000g for 10 min to collect serum, then stored at -80°C until analyzed. At backcross generation 4, serum from transgenic lines 208 and 733 was analyzed for testosterone or FSH or LH by the Ligand Assay and Analysis Core at the University of Virginia. At background generation 7, serum from all transgenic lines was analyzed by a competitive immunoassay using the Testosterone Elisa Kit (Enzo Life Sciences Inc., Farmingdale, New York) with sensitivity at 5.67pg/ml and range 7.81 - 2,000 pg/ml. The data were analyzed by using a Four Parameter Logistic Curve from MyAssays.

Estrous cycles

We compared XX and XY^{Δ} female rats, born of XY^{Δ} mothers (backcross generation 2). After approximately 8 weeks of age, vaginal smears were collected [33] and staged under a brightfield microscope. Assessment of cycle stage was continued for 3-4 cycles, and the cycle duration was averaged for each rat.

Histological analysis of sexually dimorphic spinal nuclei

Adult P59-63 rats at backcross generation 4 from line 208 were anesthetized with isoflurane and perfused with heparinized phosphate buffered saline, and then with 4% paraformaldehyde (PFA). Spinal cords from a total of 48 animals (XYWT, n = 10; XYTG, n = 10; XXTG, n = 9; XY^{Δ}, n = 6; XXWT, n = 13) were embedded in gelatin, frozen, and sectioned transversely at 40 µm. Sections were mounted on gelatin-coated slides and stained with thionin.

Number of Motoneurons. The rat Spinal Nucleus of the Bulbocavernosus (SNB) and Dorsolateral Nucleus (DLN) are discrete groups of motoneurons located in the L5/L6 spinal segments [34-36], which innervate perineal muscles involved in male sexual function. Sex differences in the number and size of motoneurons in these nuclei are known to be caused by sex differences in the secretion of testosterone perinatally [37]. For each animal, the total numbers of SNB and DLN motoneurons were estimated using the optical disector method (Stereo Investigator, MBF Bioscience, Williston, VT). Counts were made at x937.5 under brightfield illumination. SNB and DLN motoneurons were easily recognizable as large, darkly staining, multipolar cells. In the SNB, a counting frame (110 µm X 80 µm) was moved systematically throughout a midline area (~500 µm x ~300 µm) just ventral to the central canal. For the DLN, the counting frame (~500 µm x ~500 µm) was moved along the lateral margin of the ventral horn. Only motoneurons in which there was a clear nucleus and nucleolus were counted, provided that they did not contact the forbidden lines of the counting frame. Motoneuron nucleoli were counted as they appeared while focusing through the z-axis, and nucleoli in the first focal plane (i.e., "tops") were excluded to avoid double counting. The length of the disector was approximately 16 µm, which was adequate for visualizing nucleoli in multiple focal planes. Motoneuron counts in the SNB were derived from a mean of 16.1 sections spaced 160 µm apart and distributed uniformly through the entire rostrocaudal extent of the SNB, or in the DLN from a mean of 15.6 sections spaced 160 µm apart. This sampling scheme produced an average of estimated coefficient of error (CE) of 0.09 for the SNB and 0.07 for the DLN. Cell counts for each animal were corrected for the proportion of sections sampled.

Soma size. The cross-sectional area of SNB and DLN motoneuronal somata was assessed using the Nucleator method with Stereo Investigator. A set of four rays emanating from a point randomly chosen within each motoneuron soma was drawn and oriented randomly. Soma areas of an average of 41.7 SNB and 22.9 DLN motoneurons were measured for each animal at a final magnification of x780 under brightfield illumination; average estimated coefficient of error (CE) was 0.01 for SNB and 0.02 for DLN. Soma areas within each animal were then averaged for statistical analysis.

Histological analysis of limbic brain regions

Immunohistochemistry of the Sexually Dimorphic Nucleus of the Preoptic Area (SDN-POA). The Sexually Dimorphic Nucleus of the Preoptic Area (a.k.a. caudal Medial Preoptic Nucleus) of the rat hypothalamus is a classic sexual dimorphism in a brain region controlling sexual function [38]. The sex difference is caused by perinatal sex difference in the levels of gonadal hormones [39]. Adult rats from line 208 at backcross generation 4 were anesthetized with isoflurane at P60-65 and perfused with saline and the 4% paraformaldehyde. Brains were removed, post-fixed with 4% paraformaldehyde (PFA), sectioned transversely at 40 µm. Sections were incubated in a primary antibody cocktail solution directed against calbindin (CALB, Mouse Monoclonal Anti-Calbindin-D-28K (Cat #C9848, Sigma, St. Louis, MO)) with a 1:10,000 dilution in 2% normal horse serum, 0.4% Triton X-100, and TBS for 48-72 hours at room temperature. Sections were then washed and placed in a solution of secondary antibody, biotinylated horse anti-mouse immunoglobulin G (IgG) (1:500, Vector Labs, Burlingame, CA), for 60 minutes at room temperature. The signal was developed using an avidin-biotin complex kit (Vector Labs, Burlingame, CA) and enhanced using DAB/cobalt chromagen (Sigma).

Immunohistochemistry of the Anteroventral Periventricular Nucleus (AVPV). The AVPV is a sexually dimorphic region of the rat hypothalamus controlling ovulation, which is larger in females because of the effects of testicular hormones [40]. Adult rats of line 208 and progeny of XY^{Δ} females were studied at P60-65 at backcross generation 8 for males and 4 for females. Perfusion and sectioning of brains were as described for the SDN-POA. The sections were incubated for 30 minutes in a blocking solution, then incubated in the primary antibody cocktail for 48-72 hours (1:1000 dilution of tyrosine hydroxylase mouse monoclonal antibody, MAB318, Millipore Sigma). The secondary antibody was biotinylated horse anti-mouse, Vector Laboratories Kit PK-4002. Signal was developed using avidin-biotin complex enhanced with DAB/cobalt.

Quantification of calbindin-immunoreactivity (CALB-ir) in the SDN-POA. SDN-POA cell number, cell size, and nucleus volume was measured at 630x magnification. The anterior commissure marked the rostral extent of the SDN-POA, and its caudal extent coincided with the onset of CALB-ir cells in the Bed Nucleus of the Stria Terminalis [41]. CALB-ir cells within the SDN-POA region were found in 5-6 sections in males and 2-3 sections in females.

Images of brain sections were captured using a Nikon camera mounted on a Leica DMRXA scope (Leica Microsystems, Wetzlar, Germany). The volume of the CALB-ir region of the SDN-POA was quantified by outlining the CALB-ir-defined nucleus and calculating the area of the nucleus on both sides of the brain in each section with ImageJ, then multiplying by section thickness (40 µm) and summing volumes of all sections. The number of CALB-ir cells was estimated using the optical disector method counting CALB-ir cells found within all sections through the nucleus, focusing through the Z axis and ignoring "tops" to avoid double counting. The total cell number was estimated as a sum of the counts collected from both hemispheres across all sections containing the SDN-POA. Mean cell size was estimated by measuring the areas of five randomly selected cells in each hemisphere in each section, resulting in 50-60 cell areas collected from the male SDN-POA and 20-30 cell areas measured from the female SDN-POA. The mean cell size was calculated for each animal from all the cells that were measured.

Quantification of tyrosine hydroxylase-immunoreactivity (TH-ir) in the AVPV. The AVPV area was visualized under a Leica brightfield microscope at 400x magnification. We measured 6 consecutive 40 µm sections, oriented by the morphology of the anterior commissure. The third section in the rostro-caudal series was the section at which the anterior commissure (AC) met at the midline [42]. TH-ir neurons were counted in two fields, each 100 by 200 µm. The ventral edge of the fields were at the junction of the third ventricle with the optic chiasm with the dorsal edge 200 µm above, and the medial edges of the fields were at the lateral edge of the third ventricle with field's lateral edge 100 µm to the side. TH-ir neurons were counted using an optical disector method, excluding neurons at the top of sections to avoid double counting.

Statistical analyses

Experimental groups were compared using a one-way analysis of variance (ANOVA) across the five genotypes (two genotypes of XY gonadal males and one each of the other three genotypes, Figure 1) with a post hoc Tukey-Kramer (TK) test for pairwise comparisons (NCSS statistical software). If the data (e.g., on adipose tissue) suggested that XX and XY groups were different, we used a two-way ANOVA with factors of sex chromosome complement (XX vs. XY) and gonadal type (testes vs. ovaries) to test for main effects with increased statistical power, relative to the one-way ANOVA. For body weight measurements across ages, we used a two-way repeated measures ANOVA with a between-factor of genotypes and repeated factor of age to study the body growth curve in 3 male groups (from lines 208, 733, 424, and 737), and 2 female groups (XXWT and XY^{Δ}) from XY^{Δ} litters. X^2 tests were used to judge distributions of genotypes. In all figures, error bars show standard error of the mean (SEM). The results of statistical tests are in Table 3.

Results

Production of transgenic and knockout lines

Integration of an *Sry* BAC clone into an autosome of XY Sprague Dawley rats produced four lines of XYTG gonadal males that were fertile (Table 2) and transmitted the transgene to XX offspring (XXTG) with testes. Each of the four transgenic lines were backcrossed to Sprague Dawley CD(001) for up to 10 generations to eliminate possible second transgenic integration sites or potential off-target anomalies in the genome. Founder 737 showed evidence of harboring a second ineffective *Sry* transgene because it fathered a small number of XXTG gonadal female offspring. These XXTG females were not present after backcross generation 3. All lines showed some anomalies in the intensity of PCR bands during genotyping in the first backcross generation, a possible indication of a second transgene, but these variations were eliminated by backcross generations 2 or 3. Line 208 produced some XYTG males with relatively small testes in backcross generation 4, but selective breeding prevented the occurrence of such animals in subsequent generations. Each transgenic line produced frequencies of genotypes that were not different from expected Mendelian frequencies (X^2 test, $p > 0.05$, Table 3A). The transgenic cross (Figure 1) produces three types of males, including the XXTG males and two types of XY males (XYWT and XYTG).

Using two unique gRNAs to target sites flanking the region of *Sry4a* and *Sry1*, we produced one mutant founder XY^{Δ} rat with ovaries that was fertile and produced both XXWT and XY^{Δ} daughters (Table 2). The backcross of the XY^{Δ} line to Sprague Dawley SD:CD males yielded similar numbers of XXWT and XY^{Δ} females, but an unexplained excess of XYWT males (X^2 test, $p < 0.0003$, Tables 2 and 3A). Characterization of ChrY in this model yielded unexpected outcomes resulting from CRISPR-Cas9 mutagenesis. Figure 2A

shows an annotated region of about 1.5-Mbp of assembled OP905629 sequence harboring 10 *Sry* genes, other ChrY genes, as well as the CRISPR guide RNA on-target and predicted off-target CRISPR sites (OS1-9, Figure 2A). It is not clear whether Sprague Dawley rats harbor the *Sry3* gene, which would presumably be located outside this region. Because of numerous segmentally duplicated *Sry* gene regions, many paired-end reads aligned to multiple locations, complicating detection of deleted sequences, so we used UniqueKMER [43] to identify truly unique sequences across the OP905629 sequence. Overlay of the unique sequences plot with the WGS coverage identified at least three extended deleted regions in the Y^{Δ} chromosome ranging from ~3 to ~240 kbp indicated by low or absent read coverage and lack of reads specifically overlapping unique sequences (Figure 2D). These deletion breakpoints mapped very close to CRISPR sgRNA on-target and predicted off-target sites indicating that aberrant cleavage by SpCas9 and non-homologous end-joining (NHEJ) likely produced these deletions. Several copies of *Sry* genes, and *Rbmy*, *Ube1yb* and *Ubel1yc* fall within the deleted regions (Figure 2ACD). *Sry4, Sry3BII, Sry2* and *nonHMGSry* appear to remain intact. PCR amplification of genomic DNA from XY^{Δ} rats, using unique primer sets within *Med14y*, *Tspy1*, *nonHMGSry*, *Uba1y, Kdm5d, Eif2s3y, Uty, and Usp9y,* confirmed that these genes are present (data not shown). Thus, most or all of the broadly expressed Y genes [44] are present.

A PCR amplicon spanning multiple CRISPR sites (on- and off-target) for sgRNA4a_up and OS1-7 (see Methods) amplified a product which harbors a 22- or 24-bp deletion, depending on which target site is being amplified (Figure 2B). It is currently not possible to determine whether this small deletion represents an indel at a single site, or a joining of two ends of a larger deletion between two Cas9 cleavage sites. It is also possible that, due to the multiple simultaneous cleavage and NHEJ repair events, that the order and orientation of the remaining ChrY fragments were altered.

Gonadal histology

External genitalia of all transgenic males were comparable to WT males (Figure 3). XYWT and XYTG testes were comparable in size, but XXTG testes were smaller (Figure 3). Histological analysis showed that Sertoli cells in the XXTG testes formed seminiferous tubules but the tubules lacked germ cells (Figure 4AB), as expected and shown previously in other species [45] because a second X chromosome interferes with spermatogenesis and some Y-linked genes are required for spermatogenesis [46, 47]. Lack of germ cells leads to a reduction in cord diameter [48] and in overall testis size as observed in other models of Sertoli-cell only syndrome [49]. All other gonadal cell types seen in the XYWT testes (such as the Leydig cells, myoid cells and blood cells) were observed in approximately similar numbers in the XXTG testes. The testes of XYTG males were histologically similar to XYWT males (Figure 4AB).

Histological analysis of XXWT and XY^{Δ} ovaries showed comparable morphology (Figure 4C) and all stages of oocyte development present including primary and secondary follicles, antral follicles and corpus luteum. Likewise, development and organization of granulosa and theca cells were comparable between XXWT and XY^{Δ} rats.

Analysis of Sry expression in tissues

We measured expression of *Sry* transcripts using oligo-dT primers in a reverse transcription reaction, and qPCR with primers that amplify cDNA from all *Sry* gene mRNAs except *nonHMGSry*. Adult spleen, liver and gonad were assayed in males of transgenic lines 208 and 733, and from XXWT and XY^{Δ} females (Figure 5). In all tissues, *Sry* expression varied by genotype (one-way ANOVA, $p<0.0006$, Table 3B). In spleen and liver, XYWT and XYTG males had higher levels of expression than XXTG males (TK, $p < 0.05$), possibly because of expression from ChrY that is absent in XXTG males (Figure 5AB). *Sry* was expressed from the transgene in spleen and liver as shown in XXTG males (Figure 5AB). *Sry* expression might be expected to have been higher in XYTG than XYWT in these tissues because of the additional copies of *Sry* in the transgene, but that difference was not statistically significant (TK, $p > 0.05$). *Sry* was expressed in spleen and liver of XY^{Δ} females (Figure 5), confirming the presence of functional *Sry* gene(s) on the Y^{Δ} chromosome, and suggesting that *Sry* genes remaining on the Y^{Δ} chromosome are normally expressed in those tissues in XYWT males.

In adult gonads, *Sry* was expressed in all genotypes except for XXWT females, but at much higher levels in XYTG than in other groups. The higher expression of *Sry* from XYTG testes, relative to XYWT testes, might imply that expression from the transgene was much higher than from the endogenous ChrY. However, expression from the transgene in XXTG males was quite low, undermining that simple hypothesis. Thus,

factors on ChrY and in the transgene might interact to regulate *Sry* expression in XYTG but not XXTG groups. Expression of *Sry* in ovaries of XY^{Δ} rats again attests to the presence of *Sry* on the XY^{Δ} chromosome. The expression of *Sry* in ovaries is unprecedented and perhaps paradoxical, because ovaries normally lack *Sry*. Thus, any cell type, even ovarian cells, may possess mechanisms that activate expression of *Sry* or other ChrY genes. Our analysis of XY^{Δ} indicates that *Sry2* is present on XY^{Δ} (Figure 2). *Sry2* appears to be widely expressed in many tissues of WT males [50], and may account for some of the *Sry* expression seen in Figure 5.

Growth curves

We compared the body weight increase of the four transgenic lines from 3 to 8 weeks of age (Figure 6). In general, the XXTG males grew well within the male range, but at slightly slower rates than XY groups. These differences were significant only in some lines. A repeated measures two-way ANOVA with factors of genotype (3 levels) and time (6 levels) showed a strong main effect of time ($p<0.00001$, Table 3C) in all lines, and either no effect of genotype (lines 733 or 424), or a main effect of genotype (line 737, $p=0.05$, Table 3C), or a genotype by time interaction (line 208, $p<0.0008$, Table 3C). Because the two XY genotypes (XYWT and XYTG) were not statistically different, we combined them and used a two-way ANOVA (factors of genotype (2 levels) and time (6 levels) to test for XX vs. XY differences. In line 737, the main effect of genotype was significant ($p<0.008$, Table 3C). The XX-XY difference showed a significant interaction with time in line 208 ($p<0.0003$. Table 3C), line 733 ($p<0.05$, Table 3C), and line 737 ($p<0.003$, Table 3C). In line 424, the XX-XY difference was not significant. At week 8, a comparison of the combined XY groups with the XXTG group revealed a significant difference only for line 208 ($p=0.034$, Table 3C).

Body weight of XXWT females did not differ from those of XY^{Δ} females over 3-8 weeks of age (two-way repeated measures ANOVA, Table 3C), nor at 8 weeks of age (one-way ANOVA, Table 3C).

Organ weights

In backcross generation 7, we measured weights of kidney, spleen, and testes of male genotypes in all lines (Figure 7). For all lines, testis size differed among genotypes (one-way ANOVA, $p<0.000001$, Table 3D), because testes were smaller in each line in XXTG relative to XYWT and XYTG (TK, $p<0.001$). There were no significant differences in kidney and spleen weights among the three male groups in any line (one-way ANOVA, $p>0.05$, Table 3D). Representative data are shown for line 208 in Figure 7.

We measured fat pad mass in several white adipose tissue depots in line 208 at P85-91 in gonadally intact rats fed a standard chow diet (Figure 8). Gonadal and retroperitoneal white adipose tissues (gWAT and rpWAT) represent visceral fat depots, and inguinal (iWAT) is a subcutaneous fat depot. In all three tissues, fat mass varied as a function of genotype (one-way ANOVA, $p < 0.02$, Table 3D) because of significant differences between groups with testes vs. ovaries (TK $p<0.05$) (Figure 8). For iWAT, XX rats had more fat than XY rats, within gonadal type. A two-way ANOVA with factors of sex (testes vs. ovaries) and sex chromosomes (XX vs. XY) revealed a main effect of sex ($p<0.00004$, Table 3D) and of sex chromosome complement ($p<0.05$, Table 3D).

Anogenital distance

The anogenital distance, a bioassay for prenatal levels of gonadal androgens, varied by genotype (one-way ANOVA, $p<0.00001$, Figure 9, Table 3F) reflecting the difference in AGD between rats with testes vs. ovaries. All male groups differed from all female groups (TK, $p<0.001$) but not from each other (TK, $p>0.05$). In line 737, the AGD of XXTG males was somewhat smaller than those of XYWT (TK $p<0.01$). In litters from XY^{Δ} mothers, the effect of genotype was also significant (one-way ANOVA, $p<0.00001$, Table 3F), but no significant difference was found between the two female groups (TK, $p>0.05$). The comparable AGD among same-gonad groups suggests that in all lines except 737, prenatal androgen levels are comparable among groups with testes, and among groups with ovaries.

Hormone levels

In backcross generation 4, we measured serum testosterone, LH, and FSH levels at ~P60, focusing on lines 208 and 424 (Figure 10). Serum testosterone levels did not differ significantly among male groups in each line (one-way ANOVA, $p>0.05$, Table 3G). LH levels varied significantly with genotype in line 208 (one-way ANOVA, $p<0.007$, Table 3G) because XXWT levels were significantly lower than in XYWT and XXTG males

(TK, $p<0.05$). LH levels varied significantly among genotypes in litters of XY females because of the difference between gonadal males and females (one-way ANOVA, $p<0.000002$, but did not differ between XX and XY^{Δ} females. LH levels did not differ among groups in line 424, (one-way ANOVA, $p>0.05$, Table 3G).

FSH levels in line 208 differed among the four groups (one-way ANOVA, $p<0.000001$, Table 3G). XXWT females differed from each of the male groups (TK, $p<0.005$), and the XXTG group had higher levels than XYWT or XYTG groups (TK, $p<0.01$). Similarly, FSH levels in line 424 were significantly different among genotypes (one-way ANOVA, $p<0.00001$, Table 3G). XXWT females had lower FSH levels than each of the male groups (TK, $p<0.005$), and XXTG males had higher levels of FSH than either of the other two male groups (TK, $p<0.005$). FSH levels in litters of XY^{Δ} females were significantly different among groups (one-way ANOVA $p=0.000002$, Table 3G), because each female group differed significantly from the XYWT group (TK, $p<0.001$) but not from each other.

We measured serum testosterone levels in males of all transgenic lines at backcross generation 7 (Figure 11), but found no significant differences among male groups in each line (one-way ANOVA, Table 3G).

Estrous cycles

Estrous cycle duration was measured over 3-4 complete cycles in XXWT and XY^{Δ} females [51]. Mean cycle length did not differ between these groups (XXWT: 4.69 $\pm$ 0.18 days, mean $\pm$ SEM, n=7; XY^{Δ}: 4.31 $\pm$ 0.17 days, n=6) (one-way ANOVA, $p > 0.05$, Table 3H).

Analysis of central nervous system (CNS) sexual dimorphisms: SNB, DLN, SDN-POA, and AVPV

Analysis of several brain attributes known to exhibit sexual dimorphism all showed differences between gonadal males and gonadal females. Dependent variables included the number and size of SNB and DLN motoneurons (Figures 12, 13), volume, cell number and cell size of SDN-POA CALB-ir neurons (Figure 13), and number and size of TH-ir cells in the AVPV (Figure 14). In each case, the three groups of gonadal males had comparable values for these dependent variables, which were significantly different than the values for the two groups of gonadal females, which also did not differ from each other. A one-way ANOVA revealed a significant effect of genotype in each case ($p <0.000001$, except $p <0.02$ for DLN soma size, Table 3I). Differences between all pairs of gonadal male and female groups were significant (TK, $p<0.05$), except that all pairwise group differences were not significant for DLN soma area. In that case, however, a two-way ANOVA with factors of sex chromosome complement (XX vs. XY) and gonad type (ovaries vs. testes) indicated that DLN soma size was significantly different between gonadal males and females ($p<0.001$, Table 3I) but not between XX and XY groups. No significant differences in any of these CNS variables were found when comparing XX vs. XY groups with the same type of gonads (TK, $p>0.05$). These results support the conclusion that these sexual dimorphisms in rat CNS are caused by different secretions of gonadal hormones, confirming conclusions of previous reports based on manipulations of levels of gonadal hormones in WT males and females [38, 39, 52-55]. The current analysis also found no evidence that sex chromosome complement influences these sexual dimorphisms. In addition, XYWT males also had a larger number of SNB motoneurons than XYTG males (TK $p<0.05$), raising the possibility that the transgene produces some additional effect in XY males.

Embryonic lethality and small testis size of XY^{Δ}(Sry*TG+)

We attempted to generate a single rat line that is analogous to the FCG mouse model that combines the Y^{Δ} chromosome with the autosomal *Sry* transgene. We bred XY^{Δ} females with XYTG founders of the four transgenic lines or their descendants (Table 4). A total of 38 postnatal litters were produced, containing 350 pups. Three lines (424, 733, and 737) produced no XY^{Δ}(*Sry*TG+) gonadal male pups, although founder 737 produced one XY^{Δ}(*Sry*TG+) gonadal female pup documenting the presence of a second transgene that did not induce formation of testes, mentioned above. In line 208, 6 XY^{Δ}(*Sry*TG+) male pups were born and survived for up to a year. The frequency of XY^{Δ}(*Sry*TG+) pups in line 208 was 2.9%, much lower than the expected 16.7%. The XY^{Δ}(*Sry*TG+) males were paired with females for up to a year, but none produced any offspring. On autopsy, these males were found to have small testes that lacked sperm in histological sections (not shown).

We speculated that the combination of the transgene and Y^{Δ} chromosome was lethal during embryonic development. To evaluate that hypothesis, we generated 12 litters of embryos that were euthanized between E10 and E21 (E1 is the day after coitus). In litters at E10 fathered by founder 208 or 424, 17.2% of embryos

were XY^{Δ}(*Sry*TG+), close to the expected frequency of 16.6% (Table 4). Thus, line 424 produced this genotype at embryonic stages despite the absence of the genotype in postnatal litters. No XY^{Δ}(*Sry*TG+) embryos were found at E14 or later. These data support the conclusion that embryos were produced that possessed both the transgene and the Y^{Δ} chromosome, but that this combination resulted in embryonic lethality in all lines, which was not fully penetrant in line 208.

Discussion

We sought to develop a rat model that will allow investigation of mechanisms that contribute to sex differences in physiology and disease across a wide spectrum of disciplines. We have integrated a functional BAC *Sry* transgene into an autosome in four lines of XYTG male rats that produce XXTG offspring with testes. We have also used CRISPR technology to disrupt ChrY regions required for testis-determination, producing XY^{Δ} gonadal females that are fertile. The transgenic breeding lines produced XXTG gonadal males that can be compared to littermate XY males (XYWT and/or XYTG), to measure the differential effects of XX vs. XY sex chromosomes in a testicular hormonal environment (Figure 1, Table 1). Breeding the XY^{Δ} females to XYWT males produced XXWT and XY^{Δ} females that can be compared to measure the differential effects of XX and XY sex chromosomes in an ovarian hormonal environment. The two comparisons of XX and XY rats, with the same type of gonad, offer a unique opportunity to determine whether sex differences in any rat phenotype are the result of XX vs. XY sex chromosome complement, not mediated by gonadal secretions. The genotypes produced also allow the comparison of rats with different gonads, but with comparable sex chromosomes (either XX or XY), to determine whether sex differences in rat phenotypes are caused by gonadal hormones. These comparisons are similar (but not identical, see below) to those afforded by the Four Core Genotypes mouse model, which has been used extensively to uncover sex chromosome effects that contribute to sex differences in many mouse phenotypes [3, 4, 7]. Because rats offer advantages for study of a different set of phenotypes than mice, the advent of an FCG rat model opens the door for expanded research on sex chromosome effects. The ability to study sex chromosome effects relatively easily, in a second species, will facilitate the process of evaluating species differences and evolution of sex chromosome effects.

Functions of Sry genes

The current results contribute to an understanding of the function of some of the 11 different *Sry* genes in laboratory rats, whose diverse functions are unknown [29, 30]. The testis-determining effect of the BAC transgene indicates that *Sry4a, Sry1*, and/or *Sry3c* are sufficient, individually or in combination, to cause testis development in an XX rat. Several *Sry* genes likely are found on the Y^{Δ} chromosome, based on analysis of the chromosome sequence and expression of *Sry* in tissues from XY^{Δ} females. The remaining *Sry* genes are not sufficient by themselves to cause testis development. However, these *Sry* genes may nevertheless contribute to testis differentiation in XYWT males but require the presence of the *Sry* genes deleted from the Y^{Δ} chromosome. If the various *Sry* genes have similar functions, the formation of testes in XXTG but not XY^{Δ} groups could simply reflect a different timing or greater level of expression of *Sry* in the embryonic XXTG gonadal ridge, compared to XY^{Δ}, at the onset of testis development. Alternatively, the different encoded genes might have different functions.

Sry was expressed in adult spleen and liver in virtually all genotypes that possess the *Sry* transgene (encoding only *Sry4a*, *Sry1*, and *Sry3c*), or ChrY, or the Y^{Δ} chromosome (which lacks multiple *Sry* genes including *Sry4a*, *Sry1*, and *Sry3c*)(Figure 5). Thus, these tissues are likely to up-regulate multiple *Sry* genes normally in XYWT males. The pattern confirms previous reports of extensive expression of *Sry* in non-gonadal tissues of rats [50]. Although *Sry2* may be an *Sry* gene expressed widely or ubiquitously [50], the present results imply that it is not the only Sry gene expressed in adult tissues. Because different genotypes expressed varying levels of *Sry* in diverse tissues, and expressed different *Sry* genes (Figure 5), these variations in *Sry* expression could contribute to group differences in emergent phenotypes tested using the rat FCG model.

Comparison of rat and mouse FCG models

Although the rat FCG model and mouse FCG model both test the differential effects of XX and XY sex chromosomes, the two models have some important differences. The mouse model utilizes a single version of ChrY, which has sustained a small deletion of the region encoding the single-copy *Sry* gene [5]. Moreover, the *Sry* gene in the mouse model, when present, is encoded by the same transgene (which is present in multiple

copies [56]), with the same copy number of *Sry* in both genotypes containing *Sry*. The XX-XY comparison is similar in gonadal males and females, except for the presence of the *Sry* transgene in the gonadal males, allowing an assessment of the differences caused by sex chromosome complement. In the rat model, in contrast, the comparison of effects of XX and XY may be somewhat different in gonadal males and females, because of possible differences in the levels of *Sry* (Table 1). XX gonadal males may be compared to one or two groups of XY gonadal males, all of which differ in the copy number and type of *Sry* genes. The XYWT males have the WT ChrY with potential expression of any *Sry* gene. XXTG males have expression only of the three *Sry* genes encoded by the BAC transgene. XYTG males have potential expression of *Sry* both from the WT ChrY and from the transgene. Thus, differences in phenotype of XX and XY male groups can potentially be attributed either to the XX-XY difference, or to different doses of *Sry* if the phenotype is influenced by *Sry*. Indeed, we have detected some differences in level of *Sry* expression in tissues of various genotypes (Figure 5). Similarly, when comparing in XX and XY^{Δ} gonadal female groups, a difference in phenotype may be attributable to the complement of sex chromosomes, or the expression of *Sry* from the Y^{Δ} chromosome. Some experimental outcomes reduce the probability that differences between same-gonad XX and XY groups are caused by *Sry* dose. If, for example, XXWT and XXTG groups have the same phenotype, as occurs in some situations in FCG mice [18], the dose of *Sry* would seem not to be influencing the phenotype in the tissue of interest, and would not explain a difference between XXTG and XYWT rats.

The mouse and rat FCG models differ in number of genotypes produced and breeding schemes. In mice, there are 4 genotypes, produced within the same litters of a single cross. Maternal or litter effects are distributed across all genotypes. In contrast, the rat FCG model produces 5 genotypes (including two types of XY gonadal males) requiring two different breeding schemes. Comparisons to detect effects of sex chromosome complement (XX vs. XY, Table 1) are within-litter. However, the comparison of rats with testes vs. ovaries (keeping sex chromosome complement equal, either XX or XY) is made across litters.

Analysis of hormones in FCG rats

The FCG model attempts to distinguish the effects two major classes of sex-biasing factors, gonadal hormones and sex chromosomes. Separating the two types of effects works best if same-gonad XX and XY rats have similar levels of gonadal hormones, so that group differences in hormone levels do not confound differences caused by sex chromosome complement. We used several approaches to compare levels and effects of gonadal hormones in the rat FCG model. (1) We found that AGD was similar in XX and XY gonadal males for three of four transgenic lines (208, 733, and 424), and similar XX and XY gonadal females (Figure 9). This result implies that prenatal levels of androgens, which cause the sex difference in AGD [57-59], are comparable in these lines. Thus, the long-lasting prenatal “organizational” effects of testicular androgens, which cause numerous sex differences in non-gonadal phenotypes [60], are likely comparable in XX and XY gonadal males. The exception was line 737, in which AGD was well within the male range in XXTG males but slightly lower than that of XY males. (2) Measurement of circulating levels of testosterone in adult males showed that XXTG males had comparable levels of plasma testosterone, relative to XY males, in all four lines measured at about 60 days of age (Figures 10 and 11). (3) The length of estrous cycles of XX and XY^{Δ} gonadal female rats was not different, and both showed high fertility. Because ovarian hormones directly control the progression of estrous cycles and pregnancy, the similarity of estrous cycles and reproductive competence of XY^{Δ} females suggest that the complex dynamics and feedback effects of ovarian secretions are within the normal range of XX females. (4) We examined several classic CNS sexual dimorphisms in line 208, including the SNB, DLN, SDN-POA, and AVPV (Figures 12-15), which are considered sensitive bioassays for levels of testicular hormones, because various sexually dimorphic attributes of these neural systems (cell number and size, nucleus volume) are caused by sex differences in prenatal and/or postnatal levels of testicular androgens [38, 39, 52-55]. All of these CNS regions in line 208 show a common pattern in measures of cell number, cell size, or nucleus volume; XXTG males are similar to XYWT males and strikingly more masculine than the two groups of females, which are similar to each other (Figures 12-15). This pattern suggests that the levels of hormones that cause sexual differentiation are comparable among gonadal male groups, and also in the two female groups. The one footnote to this conclusion is that for cell number in the SNB, XYTG males had slightly fewer SNB motoneurons than XYWT males, raising the possibility of a small effect of the transgene on hormone levels in XY males.

Body weight and adiposity

In rats, the large sex difference in body weight (male > female) is controlled by perinatal and adult effects of ovarian and testicular hormones that influence feeding and have effects on adipose and other tissues regulating metabolism [61-63]. For example, gonadectomy at birth eliminates sex differences in rat body weight [63]. In FCG rats studied here, animals with testes had body weights in the range typical of XYWT males, and animals with ovaries had body weights in the range of XXWT females, irrespective of sex chromosome complement, confirming the long-standing conclusion that sexual differentiation of body weight is controlled by gonadal hormones in rats. The mass of several different rat fat depots also showed large differences caused by gonadal sex, as expected. The dominance of gonadal hormones also parallels the large hormonal effects found in FCG mice [18].

Our previous studies with FCG mice [8, 18] uncovered a large sex chromosome effect on body weight and adiposity (XX>XY, in the opposite direction from gonadal effects). We asked here for the first time if these phenotypes are influenced by sex chromosome complement. The pattern of body weights across genotypes differed from that seen in FCG mice. In all transgenic rat lines, XXTG males weighed slightly less than XYWT or XYTG males, although the difference was statistically significant only in some lines (Figure 6). In litters from XY^{Δ} females, XXWT females weighed less than XY^{Δ} females, although the difference was not statistically significant. Unlike the difference in body weight, the XX>XY difference in fat depot was in the same direction as the sex chromosome effect in mice. In measures of the rat inguinal fat depot relative to body weight, the inguinal fat depot was marginally larger, relative to body weight, in XX compared to XY rats. In mice, the differential effect of XX vs. XY on body weight and adiposity was evident in gonadally intact mice, but was made more apparent by removal of circulating gonadal hormones by gonadectomy of adult mice, or by feeding mice a high-fat diet. Further work is needed to determine if the sex chromosome effect is more pronounced in gonadectomized rats, or in animals fed a high-fat diet, as we have reported in FCG mice [8, 18].

If XX rats weigh less than XY rats because of sex chromosome complement, the result could be explained by several factors. Rats may show differential effects of genes escaping X inactivation as in the mouse, where the X escapee gene *Kdm5c* is a major cause of sex chromosome effects on body weight and adiposity [8]. Alternatively, a paternal imprint on the X chromosome of XY rats, relative to the mixed parental imprint on the X chromosome of XX rats, might slow growth as it does in mouse embryos [64]. Finally, the slightly lower body weight of XXTG males could reflect a slightly lower level of testosterone in some lines, which is revealed only in some phenotypes.

Gonadotrophin levels

We detected both gonadal hormone and sex chromosome effects on LH and FSH levels (Figure 10). LH levels were higher in gonadal males than females in line 208, a result that was not confirmed in line 424 or in progeny of XY^{Δ} females. FSH levels were robustly higher in XXTG males than in XYWT or XYTG males in lines 208 and 424, a result confirming a similar difference found in FCG mice [14]. A sex chromosome effect on FSH levels was not found in female rats in the present study, in contrast to findings in FCG mice, in which XY females had higher FSH levels than XX females. The differential control of FSH levels as a function of sex chromosome complement suggests that feedback control of FSH is different in XX and XY testes, despite their similar secretion of testosterone. This finding warrants further investigation to explain the mechanisms involved.

Perspectives and Significance

Sex chromosome effects on physiology and disease are poorly understood because specialized animal models are required to discriminate them from effects of gonadal hormones. Use of the FCG mouse models have led to the discovery of sex chromosome effects contributing to numerous phenotypic sex differences in disease phenotypes once thought to be caused exclusively by gonadal hormones [4]. However, the limitation of these models to a single species prevents a broad understanding of a major type of causal mechanism of sexual differentiation. Some diseases and phenotypes are better studied in rats than mice. Generating an FCG model in rats opens the way to investigation of sex chromosome effects in a wide variety of interesting rat phenotypes in which factors protect one sex from disease more than the other sex.

Conclusions

Our initial goal was to knock out testis-determining function on the rat ChrY, and to complement the loss of function with an autosomal testis-determining transgene. As described here, we successfully created a rat Y^{Δ} chromosome that no longer specifies testis development, and generated multiple rat lines with an *Sry* transgene that successfully induces testis development in the absence of other Y genes. Together, these rat genotypes make it possible to study XX and XY rats with testes, and XX and XY rats with ovaries, which will provides unique insights into the genetic determinants of sex differences as demonstrated by numerous studies in FCG mice.

The comparison of several *Sry* transgenic lines provides the opportunity to choose a line that is most suitable for testing for sex chromosome effects in future studies. Based on our current observations, lines 208 and 733 are most attractive. Line 424 produces smaller litters (Table 2). Line 737 is less attractive because 737 XXTG rats show a slightly smaller AGD relative to XYWT, suggesting that the XXTG testes do not produce as much androgen prenatally as XYWT testes.

Our studies have also revealed new information regarding the action of *Sry* genes in the rat. The results constrain ideas about which *Sry* genes induce rat testis differentiation. We expected that the effect of *Sry* genes would be predominantly on testis development, and were therefore surprised by the embryonic lethality when the Y^{Δ} chromosome is combined with the *Sry* transgene. Thus, the manipulated regions of ChrY contain genes or regulatory regions that are not just involved in testis determination, but also are required within a specific dose range for normal embryonic development. Further research is required to understand why changing the dose of *Sry* genes, or nearby regions of ChrY, have an effect on survival of embryos. In the meantime, the current rat models are useful for investigation of mechanisms of sexual differentiation of rat phenotypes.

Keywords
Sry, testis determination, sexual differentiation, sex determination, sex chromosome effect, Four Core Genotypes, X chromosome, Y chromosome.

Declarations

Ethics approvals. All experiments were approved by the Institutional Animal Care and Use Committees of participating institutions.

Consent for publication. Not applicable

Availability of data and materials. The datasets used during the current study are available from the corresponding author on reasonable request.

Competing interests. The authors declare no competing interests.

Funding. Supported by NIH grants OD026560 to APA, MRD, & AMG, OD030496 to APA, MRD, AMG, & VRH, HL114474 to MRD & AMG, DK120342 to KR, and by the Australian Victorian Government's Operational Infrastructure Support Program.

Authors' contributions. Conception and design of project: APA, AMG, MRD, VRH, XC, MNG, DRS, HS, DCP, KR, WG. Data acquisition and analysis: APA, XC, MNG, JMR, DRS, TM, VAF, WG, LL, AT, CW, LV, KR, VRH, AMG; Interpretation of data: APA, XC, MNG, JMR, DRS, TM, VAF, CW, LV, KR, VRH, MRD, AMG; drafting and revising manuscript: APA, XC, MNG, JMR, DRS,TM, VAF, WG, CW, LV, HS, KR, VRH, MRD, AMG.

Acknowledgements. Thanks to the following for assistance: Robin Lovell-Badge, Ryohei Sekido, Jeremy Prokop, Haley Hrncir, Stephanie Correa, Paul E. Micevych, Laura Cortes, Margaret Mohr, Nancy Forger, Stuart Tobet, Margaret M. McCarthy, Jan Willing, Mansoureh Eghbali, Kathryn Sandberg, Julia Gong, Thom Saunders and staff of the University of Michigan Animal Model Core, and the Monash University Histology Platform.

References

1. Arnold AP. A general theory of sexual differentiation. J Neurosci Res. 2017;95:1-2:291-300; doi:10.1002/jnr.23884.

2. De Vries GJ, Rissman EF, Simerly RB, Yang LY, Scordalakes EM, Auger CJ, et al. A model system for study of sex chromosome effects on sexually dimorphic neural and behavioral traits. J Neurosci. 2002;22:20:9005-14;

3. Arnold AP. X chromosome agents of sexual differentiation. Nat Rev Endocrinol. 2022; doi:10.1038/s41574-022-00697-0.

4. Arnold AP. Four Core Genotypes and XY* mouse models: Update on impact on SABV research. Neurosci Biobehav Rev. 2020;119:1-8; doi:10.1016/j.neubiorev.2020.09.021.

5. Lovell-Badge R, Robertson E. XY female mice resulting from a heritable mutation in the primary testis-determining gene, Tdy. Development. 1990;109:635-46.

6. Mahadevaiah SK, Odorisio T, Elliott DJ, Rattigan A, Szot M, Laval SH, et al. Mouse homologues of the human AZF candidate gene RBM are expressed in spermatogonia and spermatids, and map to a Y chromosome deletion interval associated with a high incidence of sperm abnormalities. Hum Mol Genet. 1998;7:4:715-27.

7. Burgoyne PS, Arnold AP. A primer on the use of mouse models for identifying direct sex chromosome effects that cause sex differences in non-gonadal tissues. Biol Sex Differ. 2016;7:68; doi:10.1186/s13293-016-0115-5.

8. Link JC, Wiese CB, Chen X, Avetisyan R, Ronquillo E, Ma F, et al. X chromosome dosage of histone demethylase KDM5C determines sex differences in adiposity. Journal of Clinical Investigation. 2020;130:11:5688-702; doi:10.1172/jci140223.

9. Itoh Y, Golden LC, Itoh N, Matsukawa MA, Ren E, Tse V, et al. The X-linked histone demethylase Kdm6a in CD4+ T lymphocytes modulates autoimmunity. J Clin Invest. 2019;130:3852-63; doi:10.1172/JCI126250.

10. Davis EJ, Broestl L, Abdulai-Saiku S, Worden K, Bonham LW, Minones-Moyano E, et al. The second X chromosome confers resilience against Alzheimer's disease-related deficits in male and female mice. Science Translational Medicine. 2020;12:558:eaaz5677; doi:10.1126/scitranslmed.aaz5677.

11. Cunningham CM, Li M, Ruffenach G, Doshi M, Aryan L, Hong J, et al. Y-Chromosome Gene, Uty, Protects Against Pulmonary Hypertension by Reducing Proinflammatory Chemokines. Am J Respir Crit Care Med. 2022; doi:10.1164/rccm.202110-2309OC.

12. Arnold AP, Cassis LA, Eghbali M, Reue K, Sandberg K. Sex Hormones and Sex Chromosomes Cause Sex Differences in the Development of Cardiovascular Diseases. Arterioscler Thromb Vasc Biol. 2017;37:5:746-56; doi:10.1161/ATVBAHA.116.307301.

13. Chen X, Watkins R, Delot E, Reliene R, Schiestl RH, Burgoyne PS, et al. Sex difference in neural tube defects in p53-null mice is caused by differences in the complement of X not Y genes. Dev Neurobiol. 2008;68:2:265-73.

14. Corre C, Friedel M, Vousden DA, Metcalf A, Spring S, Qiu LR, et al. Separate effects of sex hormones and sex chromosomes on brain structure and function revealed by high-resolution magnetic resonance imaging and spatial navigation assessment of the Four Core Genotype mouse model. Brain Struct Funct. 2016;221:2:997-1016; doi:10.1007/s00429-014-0952-0.

15. Taylor AMW, Chadwick CI, Mehrabani S, Hrncir H, Arnold AP, Evans CJ. Sex differences in kappa opioid receptor antinociception is influenced by the number of X chromosomes in mouse. J Neurosci Res. 2022;100:1:183-90; doi:10.1002/jnr.24704.

16. Cox KH, Bonthuis PJ, Rissman EF. Mouse model systems to study sex chromosome genes and behavior: relevance to humans. Front Neuroendocrinol. 2014;35:4:405-19; doi:10.1016/j.yfrne.2013.12.004.

17. Manwani B, Bentivegna K, Benashski SE, Venna VR, Xu Y, Arnold AP, et al. Sex differences in ischemic stroke sensitivity are influenced by gonadal hormones, not by sex chromosome complement. J Cereb Blood Flow Metab. 2015;35:2:221-9; doi:jcbfm2014186 [pii];10.1038/jcbfm.2014.186 [doi].

18. Chen X, McClusky R, Chen J, Beaven SW, Tontonoz P, Arnold AP, et al. The number of x chromosomes causes sex differences in adiposity in mice. PLoS Genet. 2012;8:5:e1002709; doi:10.1371/journal.pgen.1002709.

19. Vitali SH. CrossTalk opposing view: The mouse SuHx model is not a good model of pulmonary arterial hypertension. J Physiol. 2019;597:4:979-81; doi:10.1113/JP275865.

20. Gomez-Arroyo J, Saleem SJ, Mizuno S, Syed AA, Bogaard HJ, Abbate A, et al. A brief overview of mouse models of pulmonary arterial hypertension: problems and prospects. Am J Physiol Lung Cell Mol Physiol. 2012;302:10:L977-91; doi:10.1152/ajplung.00362.2011.

21. Kratchman J, Wang B, Gray G. Which is most sensitive? Assessing responses of mice and rats in toxicity bioassays. J Toxicol Environ Health A. 2018;81:7:173-83; doi:10.1080/15287394.2018.1423799.

22. Frick KM, Stillner ET, Berger-Sweeney J. Mice are not little rats: species differences in a one-day water maze task. Neuroreport. 2000;11:16:3461-5; doi:10.1097/00001756-200011090-00013.

23. Munro D, Wang T, Chitre AS, Polesskaya O, Ehsan N, Gao J, et al. The regulatory landscape of multiple brain regions in outbred heterogeneous stock rats. Nucleic Acids Res. 2022;50:19:10882-95; doi:10.1093/nar/gkac912.

24. Takeo T, Nakao S, Mikoda N, Yamaga K, Maeda R, Tsuchiyama S, et al. Optimized protocols for sperm cryopreservation and in vitro fertilization in the rat. Lab Anim (NY). 2022;51:10:256-74; doi:10.1038/s41684-022-01053-5.

25. Pattee J, Vanderlinden LA, Mahaffey S, Hoffman P, Tabakoff B, Saba LM. Evaluation and characterization of expression quantitative trait analysis methods in the Hybrid Rat Diversity Panel. Front Genet. 2022;13:947423; doi:10.3389/fgene.2022.947423.

26. Shimoyama M, Smith JR, Bryda E, Kuramoto T, Saba L, Dwinell M. Rat Genome and Model Resources. ILAR J. 2017;58:1:42-58; doi:10.1093/ilar/ilw041.

27. Yuan Y, Deng Q, Wei X, Liu Y, Lan Q, Jiang Y, et al. The Chromatin Accessibility Landscape of Adult Rat. Front Genet. 2021;12:651604; doi:10.3389/fgene.2021.651604.

28. Lanigan TM, Kopera HC, Saunders TL. Principles of Genetic Engineering. Genes (Basel). 2020;11:3; doi:10.3390/genes11030291.

29. Prokop JW, Underwood AC, Turner ME, Miller N, Pietrzak D, Scott S, et al. Analysis of Sry duplications on the Rattus norvegicus Y-chromosome. BMC Genomics. 2013;14:792; doi:10.1186/1471-2164-14-792.

30. Prokop JW, Chhetri SB, van Veen JE, Chen X, Underwood AC, Uhl K, et al. Transcriptional analysis of the multiple Sry genes and developmental program at the onset of testis differentiation in the rat. Biol Sex Differ. 2020;11:1:28; doi:10.1186/s13293-020-00305-8.

31. Howe K, Dwinell M, Shimoyama M, Corton C, Betteridge E, Dove A, et al. The genome sequence of the Norway rat, Rattus norvegicus Berkenhout 1769. Wellcome Open Res. 2021;6:118; doi:10.12688/wellcomeopenres.16854.1.

32. Bancroft JDG, M. . Theory and Practice of Histological Techniques. 6th Edition ed. 2008.

33. Ajayi AF, Akhigbe RE. Staging of the estrous cycle and induction of estrus in experimental rodents: an update. Fertil Res Pract. 2020;6:5; doi:10.1186/s40738-020-00074-3.

34. Schroder HD. Organization of the motoneurons innervating the pelvic muscles of the male rat. Journal of Comparative Neurology. 1980;192:567-87.

35. McKenna KE, Nadelhaft I. The organization of the pudendal nerve in the male and female rat. Journal of Comparative Neurology. 1986;248:532-49.

36. Breedlove SM, Arnold AP. Hormone accumulation in a sexually dimorphic motor nucleus of the rat spinal cord. Science. 1980;210:564-6.

37. Sengelaub DR, Forger NG. The spinal nucleus of the bulbocavernosus: firsts in androgen-dependent neural sex differences. Horm Behav. 2008;53:5:596-612; doi:S0018-506X(07)00272-3 [pii];10.1016/j.yhbeh.2007.11.008 [doi].

38. Gorski RA, Gordon JH, Shryne JE, Southam AM. Evidence for a morphological sex difference within the medial preoptic area of the rat brain. Brain Research. 1978;148:333-46.

39. Arnold AP, Gorski RA. Gonadal steroid induction of structural sex differences in the CNS. Annual Review of Neuroscience. 1984;7:413-42.

40. Simerly RB, Swanson LW, Gorski RA. The distribution of monoaminergic cells and fibers in a periventricular preoptic nucleus involved in the control of gonadotropin release: Immunohistochemical evidence for a dopaminergic sexual dimorphism. Brain Research. 1985;330:55-64.

41. Tsukahara S, Morishita M. Sexually Dimorphic Formation of the Preoptic Area and the Bed Nucleus of the Stria Terminalis by Neuroestrogens. Front Neurosci. 2020;14:797; doi:10.3389/fnins.2020.00797.

42. Orikasa C, Kondo Y, Hayashi S, McEwen BS, Sakuma Y. Sexually dimorphic expression of estrogen receptor beta in the anteroventral periventricular nucleus of the rat preoptic area: implication in luteinizing hormone surge. Proc Natl Acad Sci U S A. 2002;99:5:3306-11; doi:10.1073/pnas.052707299.

43. Chen S, He C, Li Y, Li Z, Melancon CE. A computational toolset for rapid identification of SARS-CoV-2, other viruses and microorganisms from sequencing data. Brief Bioinform. 2021;22:2:924-35; doi:10.1093/bib/bbaa231.

44. Godfrey AK, Naqvi S, Chmatal L, Chick JM, Mitchell RN, Gygi SP, et al. Quantitative analysis of Y-Chromosome gene expression across 36 human tissues. Genome Res. 2020;30:6:860-73; doi:10.1101/gr.261248.120.

45. Delot EC, Vilain EJ. Nonsyndromic 46,XX Testicular Disorders/Differences of Sex Development. In: Adam MP, Everman DB, Mirzaa GM, Pagon RA, Wallace SE, Bean LJH, et al., editors. GeneReviews((R)). Seattle (WA)1993.

46. Vernet N, Mahadevaiah SK, Ellis PJ, de Rooij DG, Burgoyne PS. Spermatid development in XO male mice with varying Y chromosome short-arm gene content: evidence for a Y gene controlling the initiation of sperm morphogenesis. Reproduction. 2012;144:4:433-45; doi:REP-12-0158 [pii];10.1530/REP-12-0158 [doi].

47. Heard E, Turner J. Function of the Sex Chromosomes in Mammalian Fertility. Cold Spring Harb Perspect Biol. 2011;10:a002675.

48. Liu B, Liu C, Ma B, Zhang R, Zhao Z, Xiao S, et al. PA1 participates in the maintenance of blood-testis barrier integrity via cooperation with JUN in the Sertoli cells of mice. Cell Biosci. 2022;12:1:41; doi:10.1186/s13578-022-00773-y.

49. Wang Z, Xu X, Li JL, Palmer C, Maric D, Dean J. Sertoli cell-only phenotype and scRNA-seq define PRAMEF12 as a factor essential for spermatogenesis in mice. Nat Commun. 2019;10:1:5196; doi:10.1038/s41467-019-13193-3.

50. Prokop JW, Tsaih SW, Faber AB, Boehme S, Underwood AC, Troyer S, et al. The phenotypic impact of the male-specific region of chromosome-Y in inbred mating: the role of genetic variants and gene duplications in multiple inbred rat strains. Biol Sex Differ. 2016;7:10; doi:10.1186/s13293-016-0064-z.

51. Cora MC, Kooistra L, Travlos G. Vaginal Cytology of the Laboratory Rat and Mouse: Review and Criteria for the Staging of the Estrous Cycle Using Stained Vaginal Smears. Toxicol Pathol. 2015;43:6:776-93; doi:10.1177/0192623315570339.

52. Sengelaub DR, Jordan CL, Kurz EM, Arnold AP. Hormonal control of neuron number in sexually dimorphic spinal nuclei of the rat. II. Development of the spinal nucleus of the bulbocavernosus in androgen-insensitive (Tfm) rats. Journal of Comparative Neurology. 1989;280:630-6.

53. Nordeen EJ, Nordeen KW, Sengelaub DR, Arnold AP. Androgens prevent normally occuring cell death in a sexually dimorphic spinal nucleus. Science. 1985;229:671-3.

54. Lee JH, Jordan CL, Arnold AP. Critical period for androgenic regulation of soma size of sexually dimorphic motoneurons in rat spinal cord. Neurosci Lett. 1989;98:79-84.

55. Simerly RB, Swanson LW, Handa RJ, Gorski RA. The influence of perinatal androgen on the sexually dimorphic distribution of tyrosine-hydroxylase immunoreactive cells and fibers in teh anteroventral periventricular nucleus of the rat. Neuroendocrinology. 1985;40:501-9.

56. Itoh Y, Mackie R, Kampf K, Domadia S, Brown JD, O'Neill R, et al. Four core genotypes mouse model: localization of the Sry transgene and bioassay for testicular hormone levels. BMC Res Notes. 2015;8:69; doi:10.1186/s13104-015-0986-2.

57. Wolf CJ, Hotchkiss A, Ostby JS, LeBlanc GA, Gray LE, Jr. Effects of prenatal testosterone propionate on the sexual development of male and female rats: a dose-response study. Toxicol Sci. 2002;65:1:71-86; doi:10.1093/toxsci/65.1.71.

58. McIntyre BS, Barlow NJ, Foster PM. Androgen-mediated development in male rat offspring exposed to flutamide in utero: permanence and correlation of early postnatal changes in anogenital distance and nipple retention with malformations in androgen-dependent tissues. Toxicol Sci. 2001;62:2:236-49; doi:10.1093/toxsci/62.2.236.

59. Bowman CJ, Barlow NJ, Turner KJ, Wallace DG, Foster PM. Effects of in utero exposure to finasteride on androgen-dependent reproductive development in the male rat. Toxicol Sci. 2003;74:2:393-406; doi:10.1093/toxsci/kfg128.

60. Arnold AP. The organizational-activational hypothesis as the foundation for a unified theory of sexual differentiation of all mammalian tissues. Horm Behav. 2009;55:5:570-8.

61. Asarian L, Geary N. Sex differences in the physiology of eating. Am J Physiol Regul Integr Comp Physiol. 2013;305:11:R1215-R67; doi:ajpregu.00446.2012 [pii];10.1152/ajpregu.00446.2012 [doi].

62. Nance DM, Gorski RA. Neurohormonal determinants of sex differences in the hypothalamic regulation of feeding behavior and body weight in the rat. Pharmacol Biochem Behav. 1975;3:1 Suppl:155-62.

63. Slob AK, Van der Werff Ten Bosch JJ. Sex differences in body growth in the rat. Physiol Behav. 1975;14:3:353-61; doi:10.1016/0031-9384(75)90044-x.

64. Thornhill AR, Burgoyne PS. A paternally imprinted X chromosome retards the development of the early mouse embryo. Development. 1993;118:1:171-4; doi:10.1242/dev.118.1.171.

Table 1: Contrasts Among Genotypes

Cross	Progeny	Genotype	Gonad	PAR	NPX	NPY	*Sry*	Contrasts
transgenic	XYWT	XY WT	M	2	1	1	WT + TG	XXTG vs. XYWT shows effects of sex chromosome complement and *Sry* dose
XX x XYTG	XYTG	XY(*Sry* TG+)	M	2	1	1	TG	XXTG vs. XYTG shows effects of sex chromosome complement and *Sry* dose
	XXTG	XX(*Sry* TG+)	M	2	2	0	TG	XYTG vs. XYWT shows effect of *Sry* dose
	XXWT	XX WT	F	2	2	0	0	XXTG vs. XXWT shows effects of gonad and *Sry*
								XXWT vs. XYWT shows effects of sex chromosome complement and gonad
knockout	XXWT	XX WT	F	2	2	0	0	XXWT vs. XYΔ shows effect of sex chromosome complement including *Sry dose*
XYΔ x XYWT	XYF	XY^{Δ}	F	2	1	Y^{Δ}	Y^{Δ}	XXWT vs. XYWT shows effects of sex chromosome complement and gonad
	XYWT	XY WT	M	2	1	1	WT	XYΔ vs. XYWT shows effect of gonad and *Sry* dose

Table 2. Frequencies of Genotypes

Line	Generations	Number of litters	Mean litter size	Distribution of Genotypes			
				XXWT	**XYWT**	**XXTG**	**XYTG**
208	4 through 9	24	12.1	28.4%	27.7%	18.7%	25.4%
733	4 through 9	10	13.4	29.4%	21.4%	27.0%	22.2%
424	4 through 8	15	9	32.6%	19.4%	27.1%	20.8%
737	4 through 7	10	11.2	21.9%	27.6%	25.7%	24.8%
				XXWT	**XYWT**	**XYΔ**	
XYΔ	2 through 7	39	12	24.5%	45.4%	30.2%	

Table 3. Results of Statistical Tests

Abbreviations: DV, dependent variable; 2WA, two-way ANOVA; 1WA, one-way ANOVA, T, time; G, genotype; SCC, SCC, sex chromosome complement (XX vs. XY), df, degrees of freedom, * p<0.05 or better.

				Chi Square	**df**	**n**	**p**	
A	genotype frequencies	Chi Square	208	3..6853	3	288	0.298	
			733	1.0976	3	126	0.778	
			424	3.1233	3	144	0.373	
			737	0.3614	3	105	0.948	
			XYΔ	16.4	2	489	0.000275*	
	DV	**test**	**line**	**factors**	**df**	**F-ratio**	**p level**	**eta squared**
B	*Sry* expression spleen	1WA	208 and KO	G	4, 34	17.54	0.000000*	0.6735
	Sry expression liver	1WA	208 and KO	G	4, 35	22.09	0.000000*	0.7163
	Sry expression gonad	1WA	208 and KO	G	4, 33	86.89	0.000000*	0.9133
	Sry express spleen	1WA	733	G	2, 21	49.84	0.000000*	0.8260
	Sry expression liver	1WA	733	G	2, 23	10.9	0.000565*	0.5094
	Sry expression testis	1WA	733	G	2, 23	90.36	0.000000*	0.8959
C	body weight	2WA repeated	208	G	2, 175	1.53	0.230709	0.0038
	3-8 weeks			T repeated	5, 175	3515.12	0.000000*	0.9379
				G x T	10, 175	3.24	0.000731*	0.0017
	body weight	2WA repeated	733	G	2, 145	0.55	0.580526	0.0015
	3-8 weeks			T repeated	5, 145	1918.46	0.000000*	0.9361
				G x T	10, 145	1.51	0.141972	0.0015
	body weight	2WA repeated	424	G	2, 130	1.73	0.197665	0.0066
	3-8 weeks			T	5, 130	1510.17	0.000000*	0.9210
				G x T	10, 130	1.36	0.208089	0.0017
	body weight	2WA repeated	737	G	2, 155	3.33	0.049909*	0.0059
	3-8 weeks			T repeated	5, 155	1477.69	0.000000*	0.9417
				G x T	10, 155	1.81	0.064163	0.0023
	body weight	2WA repeated	208	SCC	1, 180	2.83	0.100892	0.0034
	3-8 weeks			T repeated	5, 180	2933.43	0.000000*	0.7903
				SCC x T	5, 180	5.09	0.000217*	0.0014
	body weight	2WA repeated	733	SCC	1, 150	1.08	0.307731	0.0014
	3-8 weeks			T repeated	5, 150	1635.12	0.000000*	0.7897
				SCC x T	5, 150	2.35	0.043759*	0.0011
								0.0011
	body weight	2WA repeated	424	SCC	1, 135	2.06	0.162493	0.0040
	3-8 weeks			T repeated	5. 135	1275.89	0.000000*	0.7728
				SCC x T	5, 135	1.91	0.096623	0.0012
	body weight	2WA repeated	737	SCC	1, 150	8.22	0.007507*	0.0014
	3-8 weeks			T repeated	5, 150	1387.76	0.000000*	0.7897
				SCC x T	5, 150	5	0.000290*	0.0011
	body weight	1WA	XXWT vs. XYΔ	SCC	1, 70	2.57	0.131048	0.0092
	3-8 weeks			T repeated	5, 70	305.19	0.000000*	0.8975
				SCC X T	5, 70	0.65	0.664468	0.0019
	body weight	1WA	208	SCC	1, 36	4.86	0.034029*	0.1189
	8 weeks	1WA	733	SCC	1, 30	3.05	0.090769	0.0924
		1WA	424	SCC	1, 27	2.13	0.15557	0.0733
		1WA	737	SCC	1, 30	3.13	0.086809	0.0946
		1WA	XXWT vs. XYΔ	SCC	1.14	0.16	0.694988	0.0113

Table 3. Results of Statistical Tests (continued)

	DV	test	line	factors	df	F-ratio	p level	eta squared
D	Left testis weight	1WA	208	G	2, 35	560.09	0.000000*	0.9697
		1WA	733	G	2, 29	247.81	0.000000*	0.9447
		1WA	424	G	2, 25	178.43	0.000000*	0.9345
		1WA	737	G	2, 29	108.31	0.000000*	0.8819
	kidney weight	1WA	208	G	2, 35	1.12	0.338723	0.0600
		1WA	733	G	2, 29	0.86	0.433127	0.0561
		1WA	424	G	2, 25	1.24	0.305556	0.0905
		1WA	737	G	2, 29	1.18	0.322427	0.0751
	spleen weight	1WA	208	G	2, 35	1.29	0.288274	0.0686
		1WA	733	G	2, 29	1.29	0.289433	0.0820
		1WA	424	G	2, 25	1.72	0.198785	0.1212
		1WA	737	G	2, 29	0.22	0.801667	0.0151
	gWAT	1WA	208, females	G	4, 17	4.07	0.017119*	0.4891
	rpWAT	1WA	208, females	G	4, 17	6.27	0.002732*	0.5961
	iWAT	1WA	208, females	G	4, 17	12.59	0.000061*	0.7476
	iWAT	2WA	208, females	SCC	1, 18	4.61	0.045743*	0.0695
				sex	1, 18	44.45	0.000003*	0.6708
				SCC x sex	1, 18	1.08	0.312558	0.0163
F	AGD	1WA	208	G	3, 63	274.98	0.000000*	0.9290
		1WA	733	G	3, 47	201.11	0.000000*	0.9277
		1WA	424	G	3, 60	300.8	0.000000*	0.9377
		1WA	737	G	3, 39	332.09	0.000000*	0.9623
		1WA	XYΔ litters	G	2, 39	573.86	0.000000*	0.9671
G	testosterone N4	1WA	208	G	2, 26	0.34	0.712827	0.0257
		1WA	424	G	2, 17	2.02	0.16352	0.1919
	LH	1WA	208	G	3, 33	4.89	0.006408*	0.3076
		1WA	424	G	3, 22	2.01	0.141501	0.2154
		1WA	XYΔ litters	G	2, 14	0.15	0.862874	0.0208
	FSH	1WA	208	G	3, 33	27.71	0.000000*	0.7159
		1WA	424	G	3, 25	35.96	0.000000*	0.8118
		1WA	XYΔ litters	G	2, 14	40.28	0.000002*	0.8519
	testosterone N7	1WA	208	G	2, 35	0.13	0.881618	0.0072
		1WA	733	G	2, 26	0.02	0.982399	0.0014
		1WA	424	G	2, 18	0.9	0.423858	0.0910
		1WA	737	G	2, 15	0.25	0.782673	0.0321
H	estrous cycle length	1WA	XX vs. XYΔ	G	1, 11	2.41	0.148966	0.1796
I	SNB neuron number	1WA	208	G	4, 43	71.62	0.000000*	0.8695
	SNB soma size	1WA	208	G	4, 42	76.27	0.000000*	0.8790
	DLN neuron number	1WA	208	G	4, 43	18.27	0.000000*	0.6295
	DLN soma size	1WA	208	G	4, 43	3.37	0.017467*	0.2386
	SDN-POA volume	1WA	208	G	4, 32	90.36	0.000000*	0.9187
	SDN-POA neuron number	1WA	208	G	4, 32	85	0.000000*	0.9140
	SDN-POA soma size	1WA	208	G	4, 32	94.64	0.000000*	0.9221
	AVPV neuron number	1WA	208	G	4, 35	53.76	0.000000*	0.8600
	AVPV soma size	1WA	208	G	4, 31	41.67	0.000000*	0.8432
	DLN soma size	2WA	208	SCC	1, 44	0.36	0.549963	0.0063
				sex	1, 44	12.62	0.000923*	0.2189
				SCC x sex	1, 44	0.57	0.456005	0.0098

Table 4: Genotype Frequencies from Cross of XYΔ x XYTG

	founder	# pups	# litters	litter size	XXWT	XYΔ	XYWT	XXTG	XYTG	XYΔTG
postnatal	208	210	21	9.9	21.4%	5.7%	30.5%	9.0%	30.5%	2.9%
	424	51	5	10.2	7.8%	13.7%	17.6%	19.6%	41.2%	0.0%
	733	33	5	6.6	27.3%	15.2%	27.3%	9.1%	21.2%	0.0%
	737	56	7	8	14.3%	21.4%	41.1%	5.4%	16.1%	1.8%
embryonic	age									
	E10	29	3	9.7	3.4%	6.9%	20.7%	13.8%	37.9%	17.2%
	E14	26	2	13	3.8%	15.4%	23.1%	3.8%	53.8%	0.0%
	>E16	84	7	12	6.0%	7.1%	35.7%	4.8%	46.4%	0.0%

Figure 1. Two crosses producing FCG rats. Above, the *Sry* autosomal transgene is carried by the XY(*Sry*TG+) father, which produces four types of sperm, X and Y each with or without the transgene. This cross allows comparison of three male groups, XX(*Sry*TG+) and XYWT and XY(*Sry*TG+), to measure the effects of sex chromosome complement (XX vs. XY) in animals with testes. Below, the mother is XY^{Δ} and father XYWT, producing three types of viable genotypes. The cross allows comparing XX and XY^{Δ} gonadal females to measure effects of sex chromosome complement in gonadal females. Effects of gonad or gonadal hormones are also measured by cross-litter comparisons of XX gonadal males and females, or XY gonadal males and females (Table 1). Each group comparison also involves potential differences in *Sry* expression in tissues. TG, transgene.

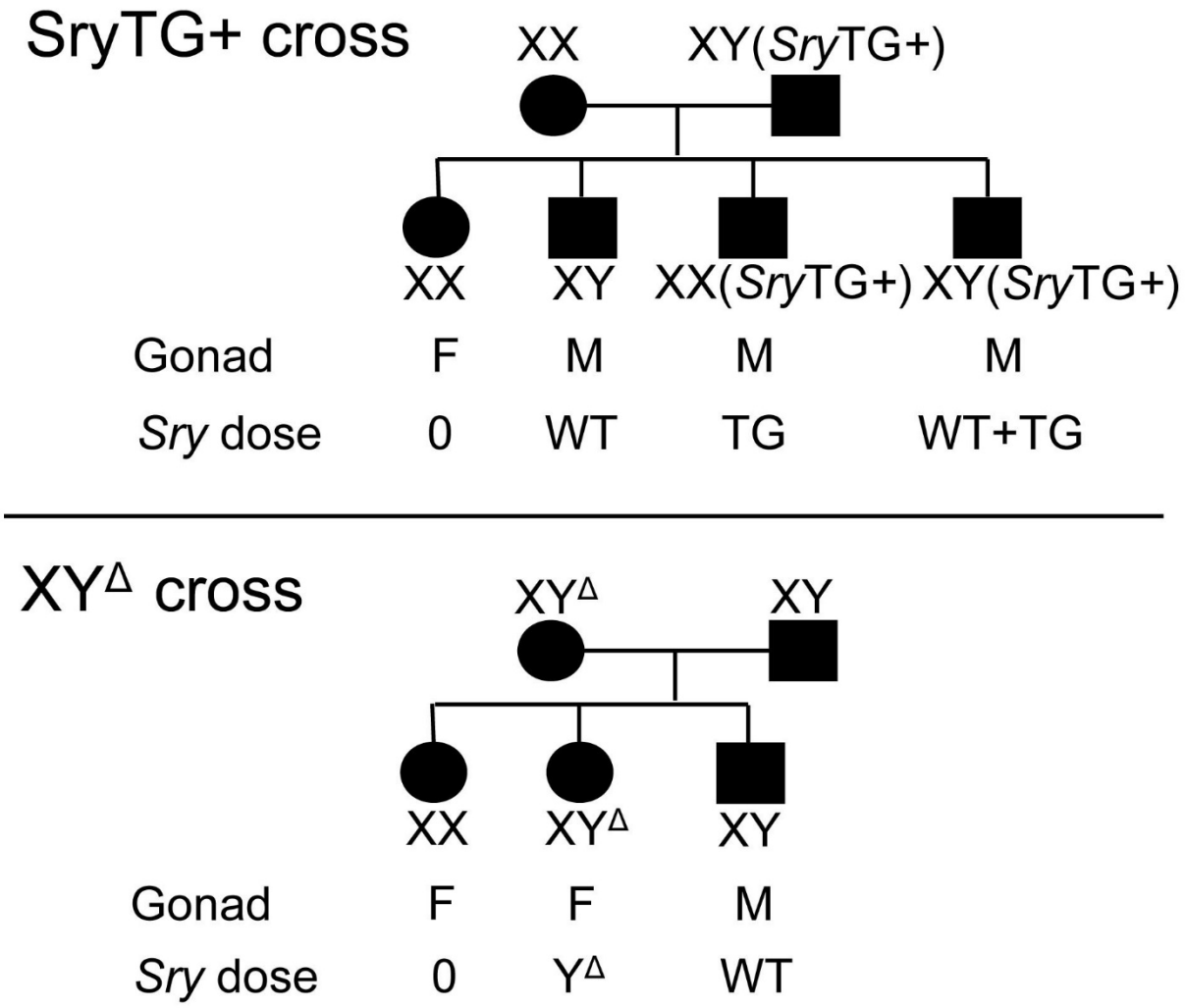

A.

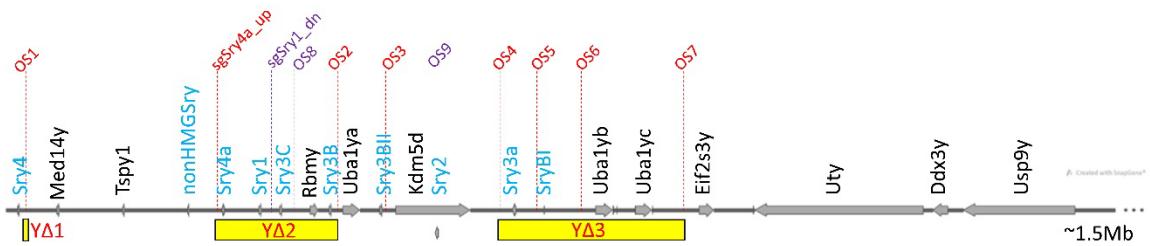

B.

```
CTGGCATGTGGGC--AGTTTCCACCTGGCAT - sgSry4a_up
CTGGCATGTGGGCAGAGTTTCCACCTGGCAT - 7 off-target sites (OS1-OS7)
CT------------------------GGCAT - 22 or 24-bp indel?

CTCACACAGCTCCTCTCTGGTAGAGGAAG - sgSry1_dn
TGTCCTCAGCTCCTCTCTGGTAGAGGAAG - 2 off-target sites (OS8, OS9)
```

C.

Deleted	*Sry4a, Sry1, Sry3C, Sry3B, Sry3a, SryBI*
Intact	*nonHMG Sry, Sry4, Sry3BII, Sry2, (Sry3?)*

D.

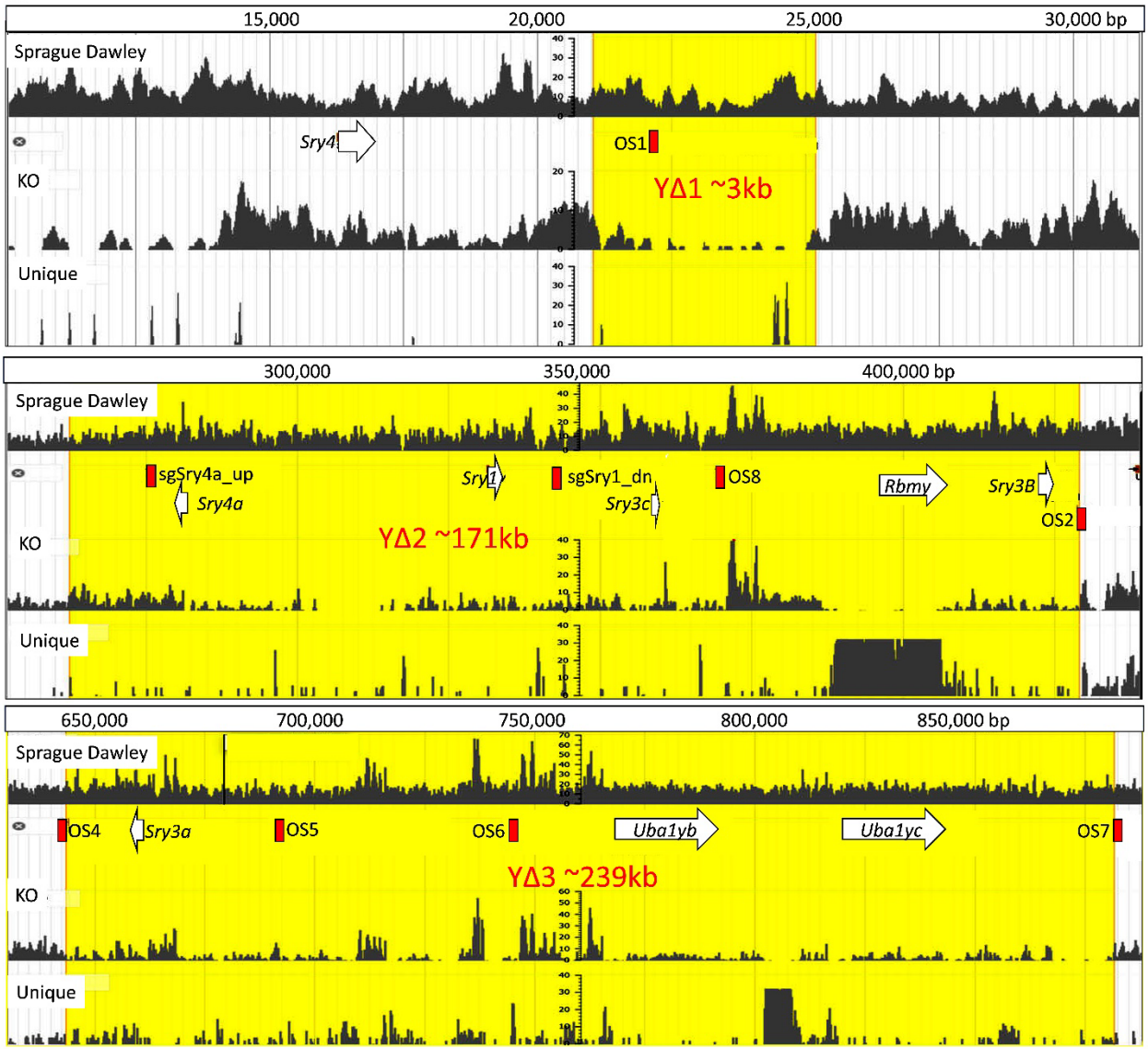

Figure 2: Characterization of the Y$^{\Delta}$ chromosome generated using CRISPR-Cas9. A. Schematic map showing the order of genes along a ~1.5Mbp region of the rat Yp chromosome, based on Genbank Accession OP905629. Ten Sry genes are shown. It is unknown if Sprague Dawley (SD) rats have an *Sry3* gene (GenBank: EU984077) in this or another region of ChrY; it has thus far only reported in SHR strain, but not the

Wistar-Kyoto (WKY) strain [29]. Positions of CRISPR target sites and off-target sites OS1-9 are shown. Putative deleted regions Y∆1-3 are shown. B) Target site sequences for the two sgRNA targets and off-target site sequences OS1-9 are aligned. The 22- or 24-bp deletion indel is shown. C) Summary of deleted and intact *Sry* genes in the XY^{Δ} strain. *Rmby, Uba1yb* and *Uba1yc* are also deleted. D) Sequence coverage of XY^{Δ} ChrY in the Y∆1-3 deleted regions based on whole genome paired-end sequencing reads. The top track is a control Sprague Dawley male, middle track XY^{Δ} coverage, and lower track is the UniqueKMER plot of unique sequences. Positions of sgRNA target sites and off-target sites near deletion breakpoints are shown. sgSry4a_up, and sgSry1_dn indicate the CRISPR sgRNA on-target alignment sites.

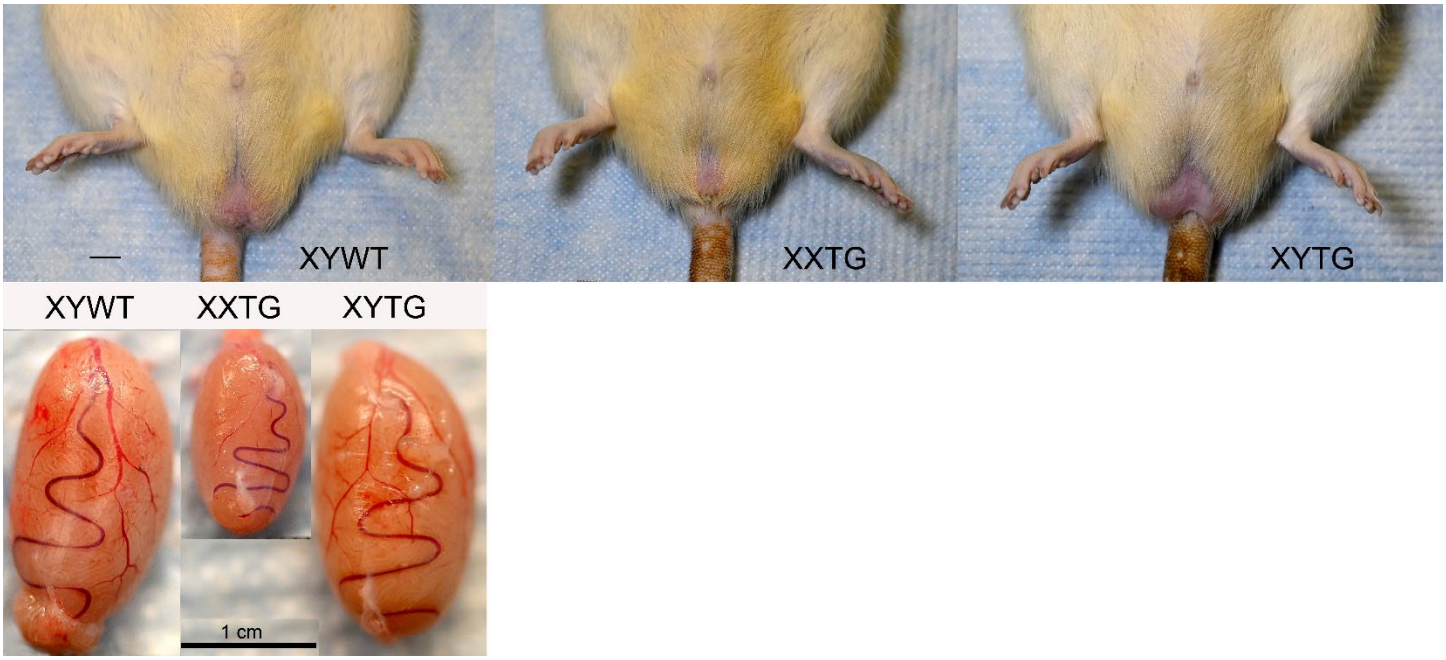

Figure 3. External genitalia and testis morphology of three types of line 208 males at postnatal day 60. Above, External genitalia of XX and XY gonadal males are comparable. Below, Testes of the three types of males. Testicular size was comparable in XYWT and XYTG males, but smaller in XXTG males. Photos from line 208 at postnatal day 60. Scale bars, 1 cm.

Figure 4. Gonadal histology. A. In transgenic lines 208 and 733, both types of XY males have comparable testicular morphology and distribution of cell types. XXTG males have seminiferous tubules and Leydig cells but lack cells in the germ cell lineage. B. Ovaries of XX and XY^{Δ} females have comparable histology. Hematoxylin and eosin staining. Scale bars are 100 μm for A and B and 200 μm for C.

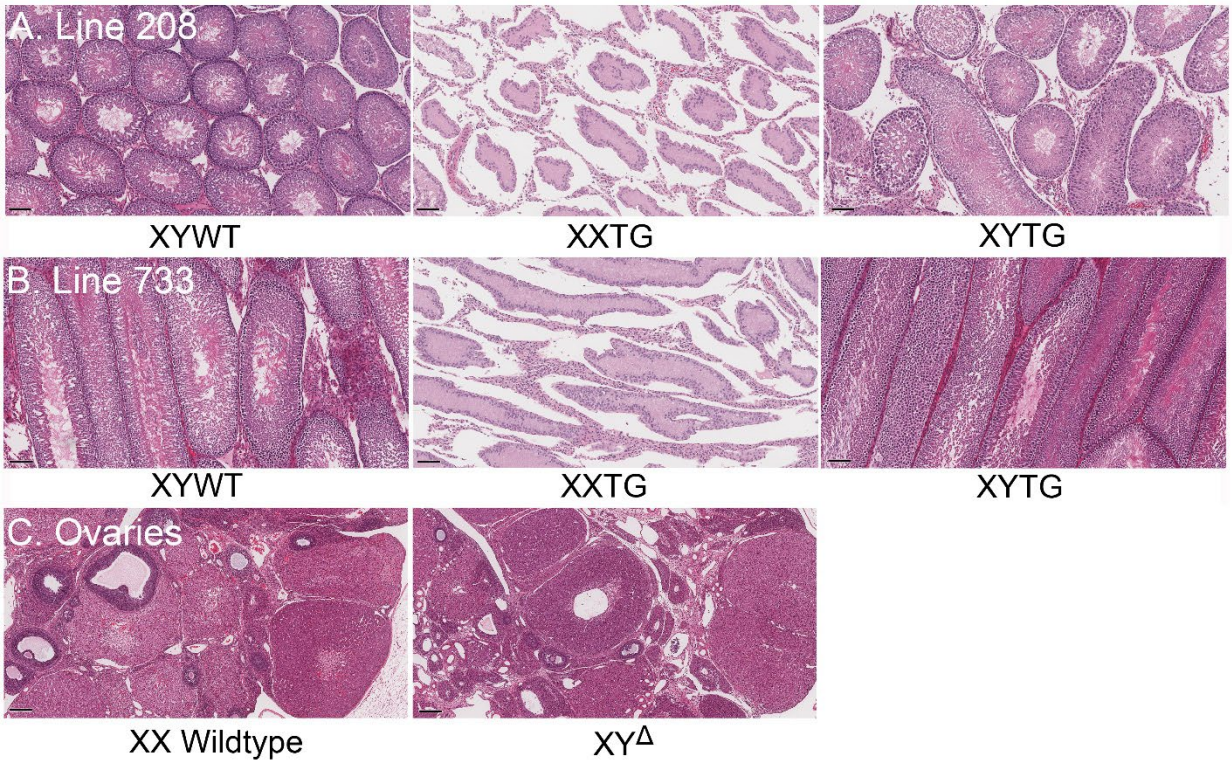

Figure 5. Expression of *Sry* mRNA in tissues measured by RTPCR. A. In transgenic line 208 and progeny of XY^{Δ} females, expression varied significantly among the five genotypes (one-way ANOVA, $p < 0.000001$). Numerous groups differed in pairwise posthoc analyses (Tukey-Kramer, $p < 0.05$) as shown by brackets. B. In transgenic line 733, three gonadal male groups showed significant variation (one-way ANOVA, $p < 0.000001$), and each group differed significantly from both of the other groups (Tukey-Kramer $p < 0.05$) as shown by brackets. In all figures, black bars depict groups with testes, and white bars depict groups with ovaries.

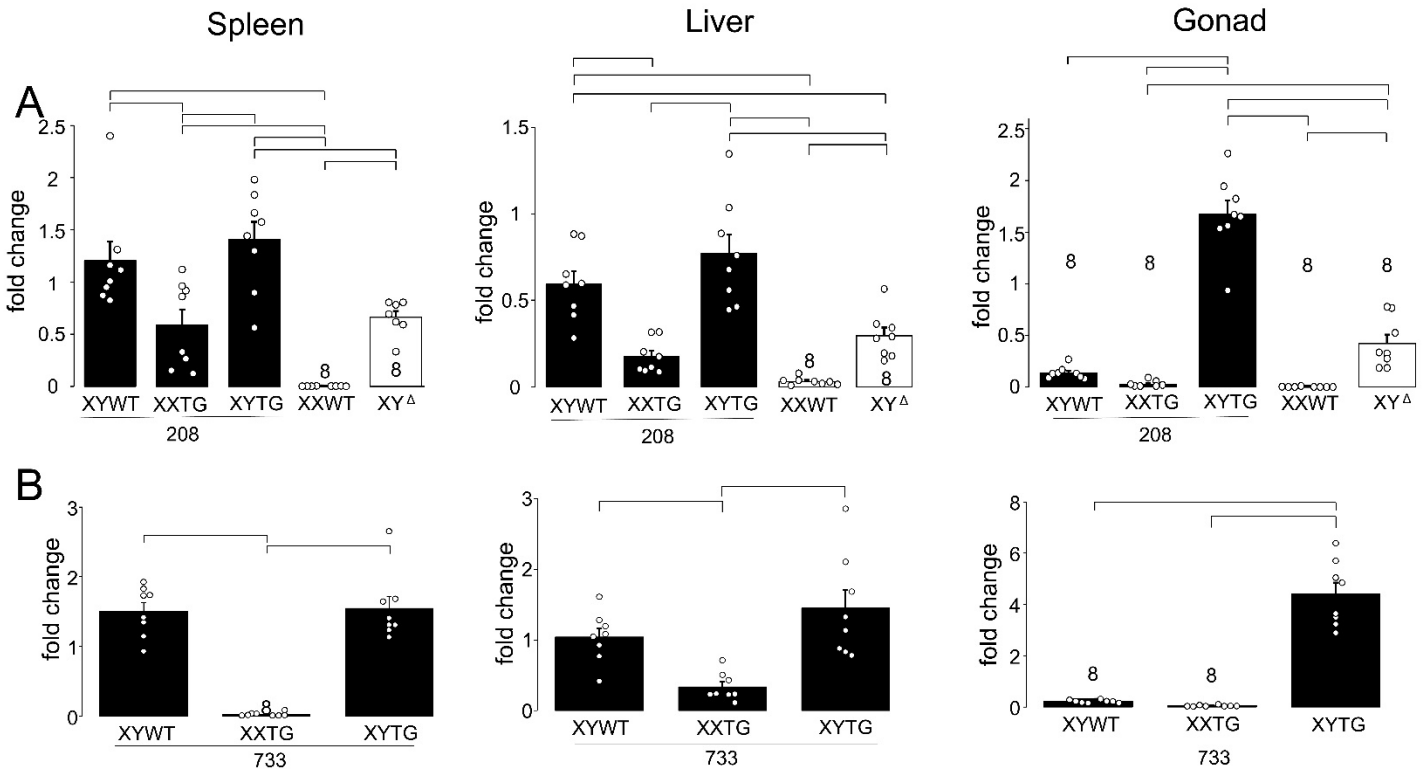

Figure 6. Growth curves. Graphs show growth in all genotypes from 3 to 8 weeks of age in backcross generation 7. XYTG males grew at rates that were not statistically different from those of XYWT males, but XXTG males grew at slightly lower rates. The two XY groups were combined for statistical comparison to XXTG males, using a two-way ANOVA with factors of sex chromosome complement (XX vs. XY) and time (repeated measure). Differences in body weight of XX and XY males were shown by a main effect of sex chromosome complement (line 733, p=0.05; line 737, p=0.008), or because of a significant interaction of sex chromosomes and time (line 208, p<0.0003); line 727, p<0.003). In line 424, no significant effect of sex chromosomes was detected. XX and XY^{Δ} females did not differ significantly in growth. Group size is indicated in parentheses.

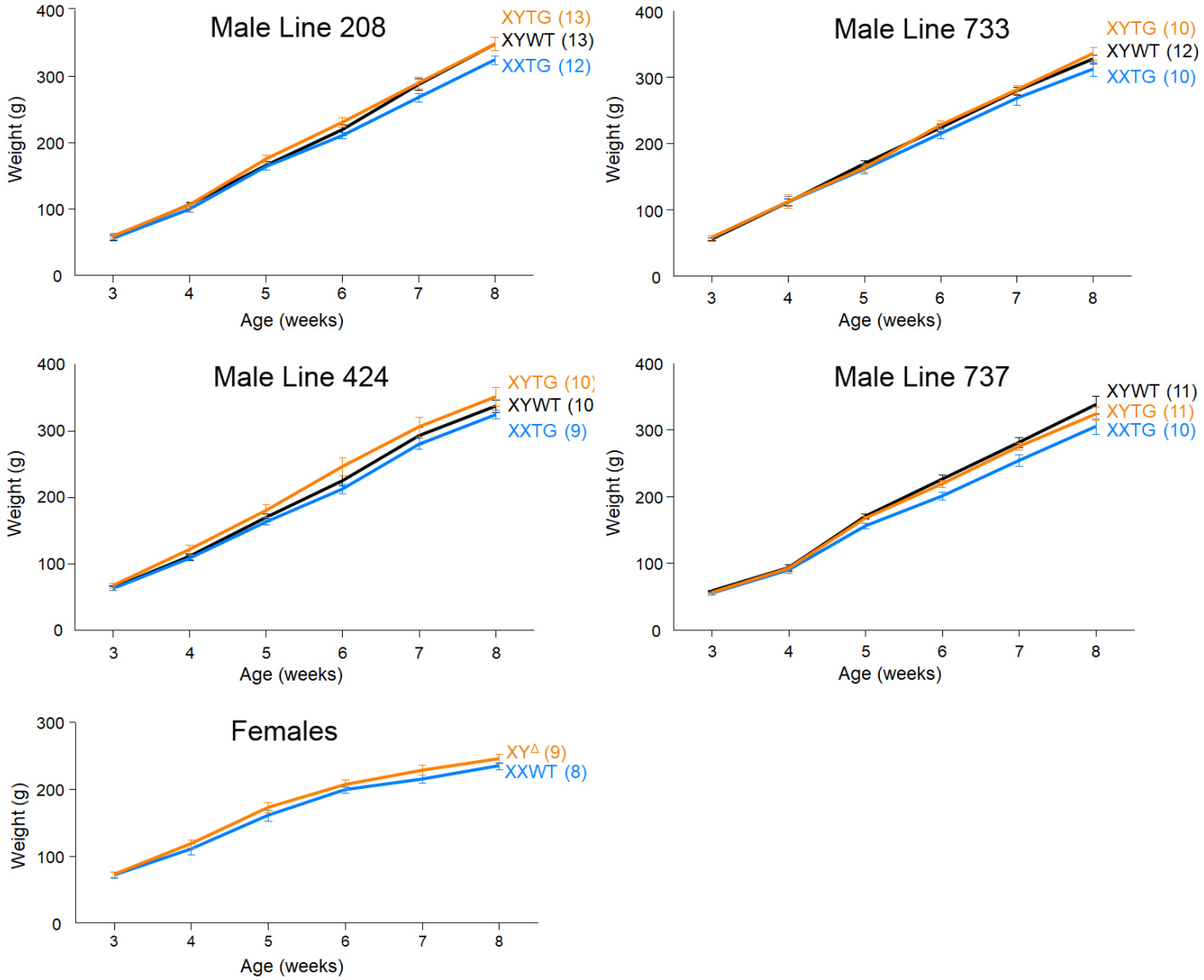

Figure 7. Organ weights. The weight of kidneys, spleens, and testes from line 208 at postnatal day 60, in backcross generation 7. There was no significant effect of genotype on kidney or spleen weight. Testis weight varied by genotype (one-way ANOVA, p<0.000001) because XXTG testes weighed significantly less than those of either XY group (*** Tukey Kramer, p<0.001). In all figures, histograms indicate mean, error bars are S.E.M., and group size is shown in each bar. NS, not significant.

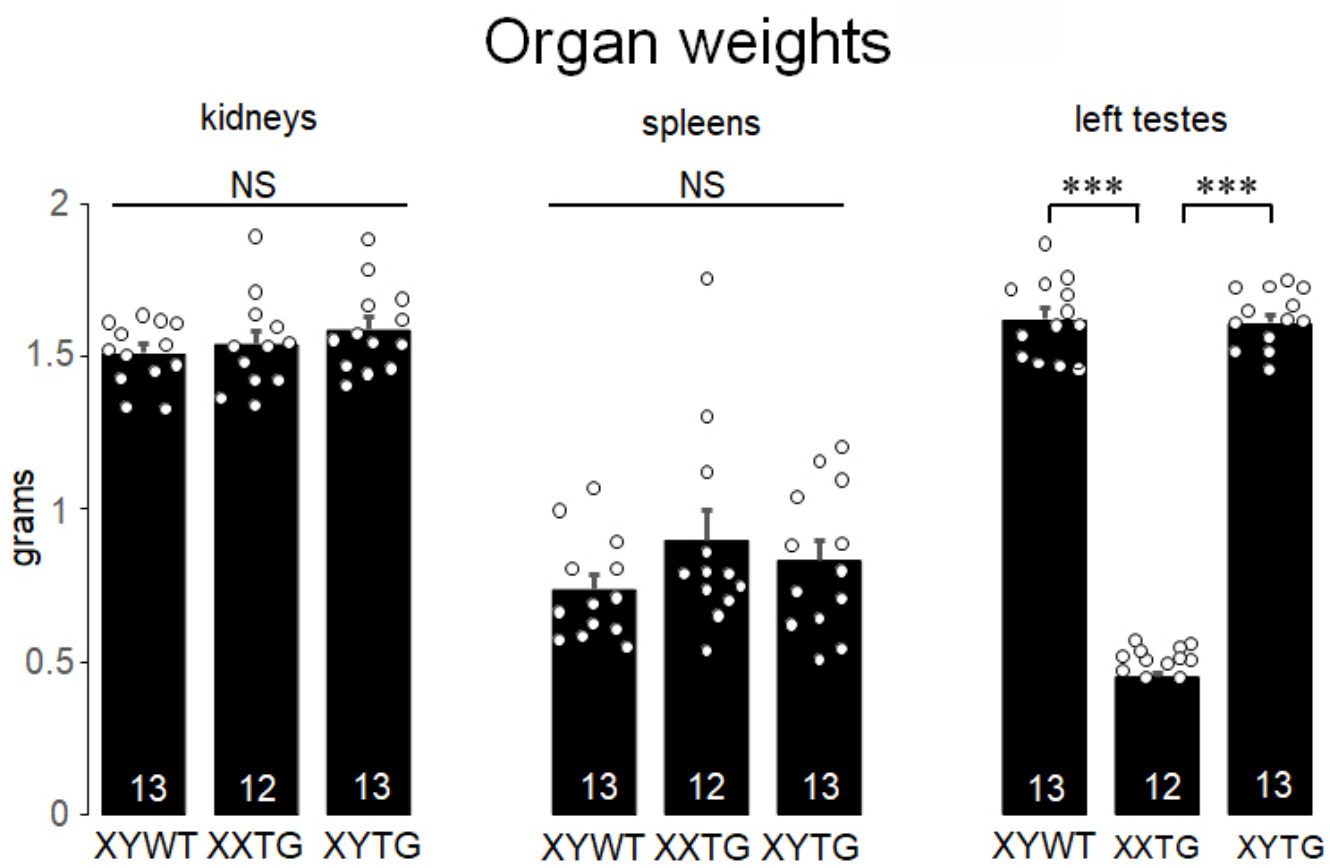

Figure 8. Weights of adipose depots. In transgenic line 208 and female progeny of XY$^{\Delta}$ females, three white adipose tissue (WAT) fat pads were weighed at P85-91: gonadal (gWAT), retroperitoneal (rpWAT), and inguinal (iWAT), and expressed as percent of body weight. All depots varied significantly among the five genotypes (one-way ANOVA, $p < 0.02$). Post hoc Tukey-Kramer tests revealed pairwise differences in weight (*, $p < 0.05$; ***, $p < 0.001$; **** $p < 0.005$). In gWAT, the weight in XYWT was greater than in either female group. In rpWAT and iWAT, the weight in XXTG rats was greater than in either female group. In iWAT, a two-way ANOVA with factors of gonad type (ovaries vs. testes) and sex chromosome complement (XX vs. XY) showed a significant main effects of gonad ($p<0.00004$) and of sex chromosome complement ($p<0.05$).

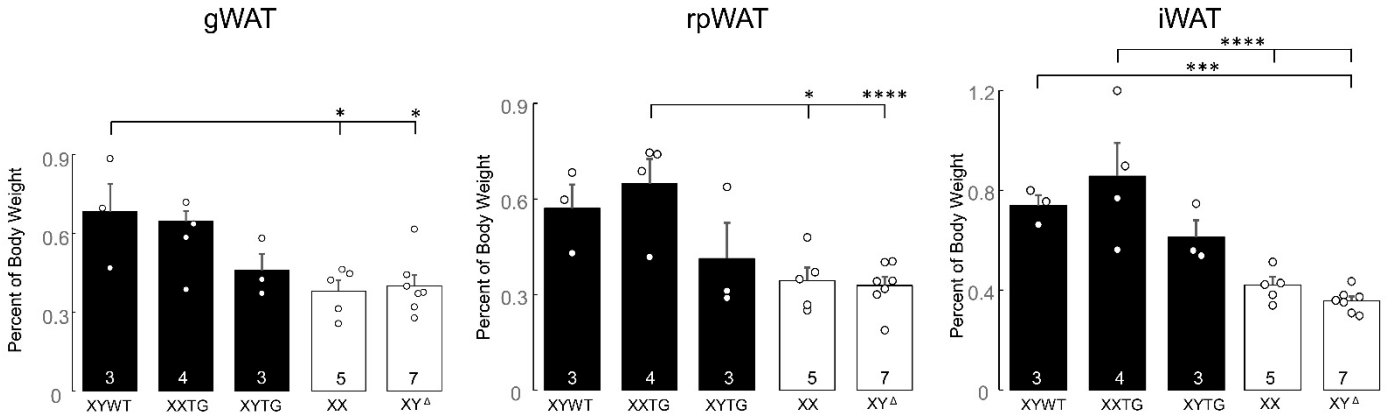

Figure 9. Anogenital distance. AGD was measured at P6-7 and expressed relative to mean AGD for XY males in the litter. In all lines, AGD differed among groups (one-way ANOVA, p<0.00001) because of a consistent difference in AGD between rats with testes or ovaries (Tukey-Kramer, p<0.001). In lines 208, 733, and 424, male genotypes did not differ in AGD. In line 737, XXTG had lower AGD than XYWT (Tukey-Kramer, **p<0.01). XX and XY gonadal females did not differ significantly in AGD. NS, not significant.

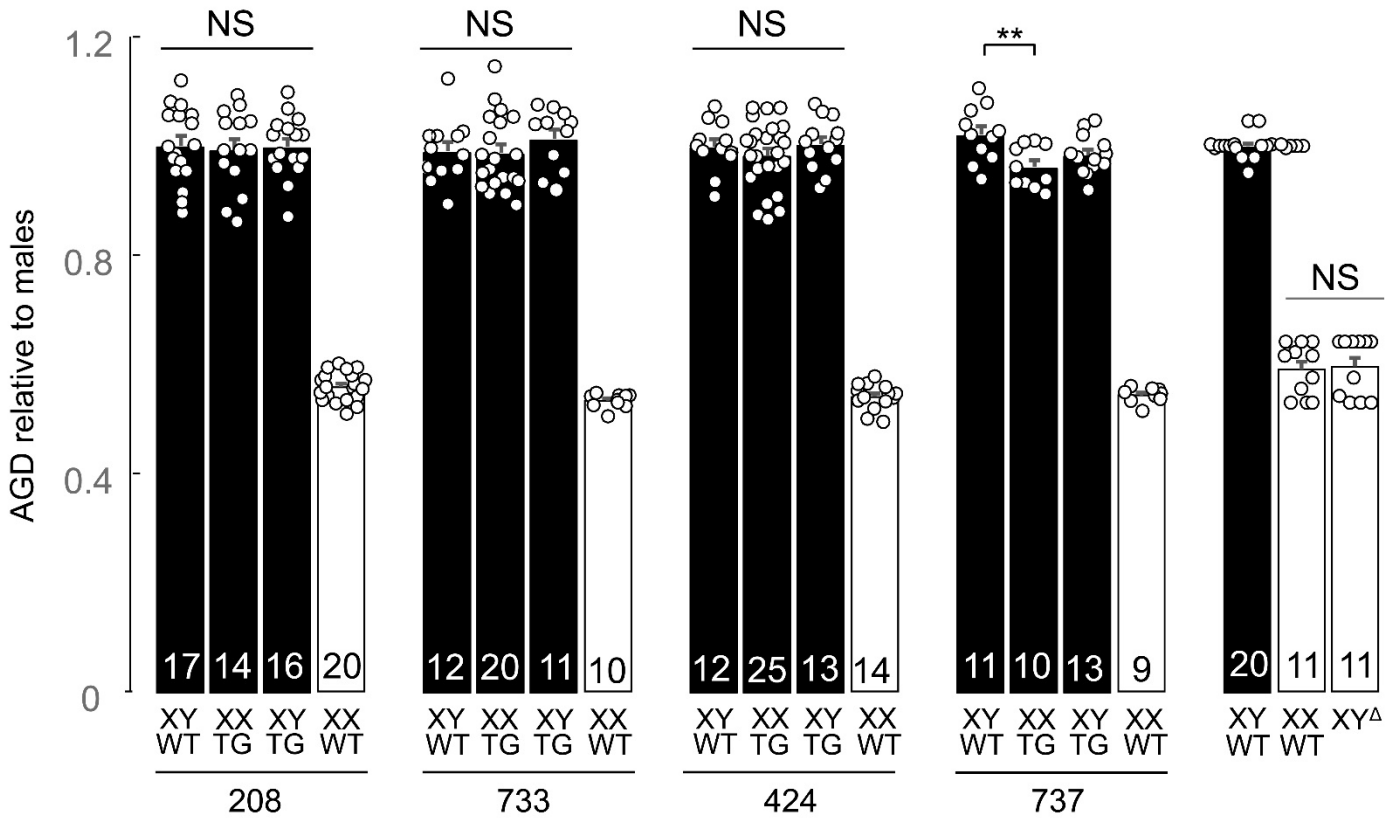

Figure 10. Levels of hormones. A., serum testosterone did not differ significantly among male groups in lines 208 or 424 (one-way ANOVA). B. LH levels did not differ significantly among groups in line 424, or among progeny of XY$^{\Delta}$ females. LH levels varied significantly with genotype in line 208 (one-way ANOVA, p<0.007) because XXWT levels were significantly lower than in XYWT and XXTG males (Tukey-Kramer, * *p*<0.05). C. FSH levels in lines 208 and 424 differed across genotypes (one-way ANOVA, † p<0.000002). XXWT females had lower levels than each of the male groups (Tukey-Kramer, p<0.005), and the XXTG group had higher levels than XYWT or XYTG groups (Tukey-Kramer, ** p<0.01). FSH levels in litters of XY$^{\Delta}$ females (right side) were significantly different among groups (one-way ANOVA † p<0.000002), because each female group differed significantly from the XYWT group (TK, *** p<0.001) but not from each other. Measurements were made in backcross generation 4 at P60. NS, not significant.

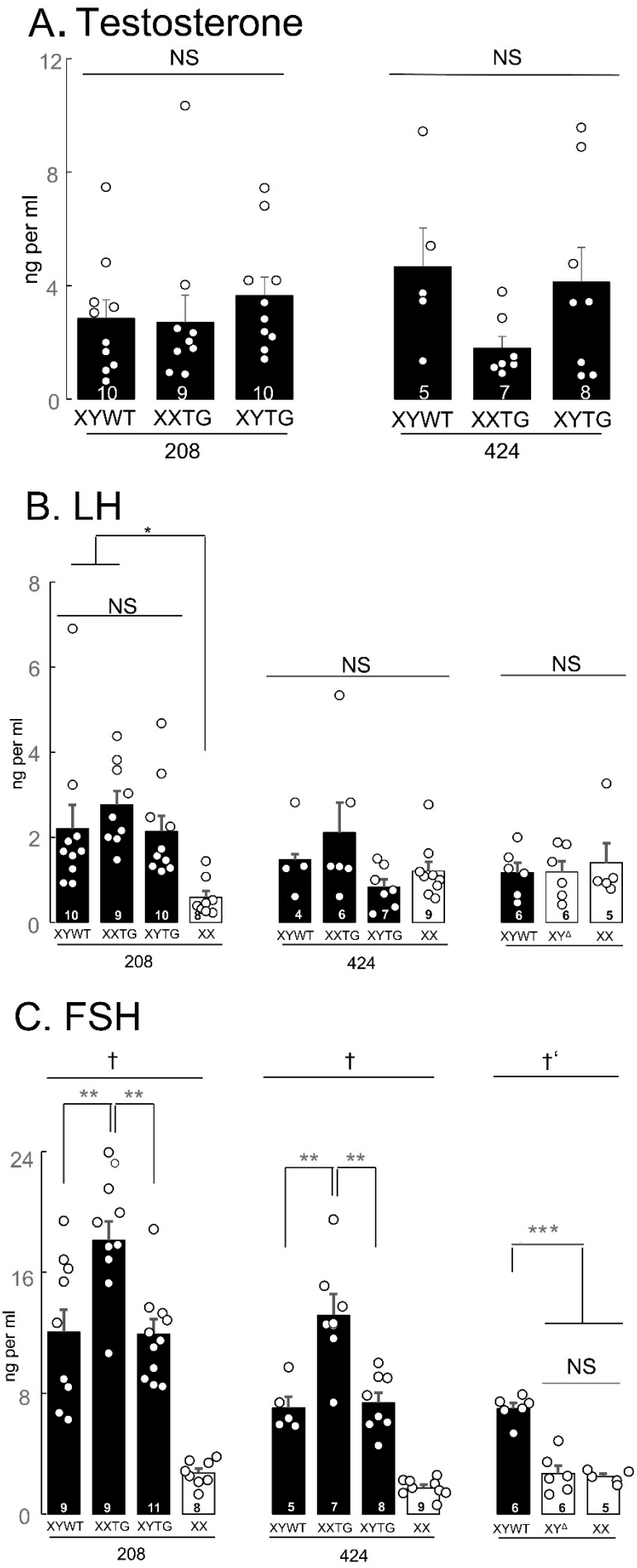
A. Testosterone
NS
NS
ng per ml
12
8
4
0
10
9
10
5
7
8
XYWT
XXTG
XYTG
XYWT
XXTG
XYTG
208
424
B. LH
*
NS
NS
NS
ng per ml
8
6
4
2
0
10
9
10
8
4
6
7
9
6
6
5
XYWT
XXTG
XYTG
XX
XYWT
XXTG
XYTG
XX
XYWT
XY^Δ
XX
208
424
C. FSH
†
†
†'
**
**
**
**
***
NS
ng per ml
24
16
8
0
9
9
11
8
5
7
8
9
6
6
5
XYWT
XXTG
XYTG
XX
XYWT
XXTG
XYTG
XX
XYWT
XY^Δ
XX
208
424

Figure 11. Serum testosterone in backcross generation 7 at P60. No significant differences (NS) were found among genotypes in all transgenic lines (one-way ANOVA).

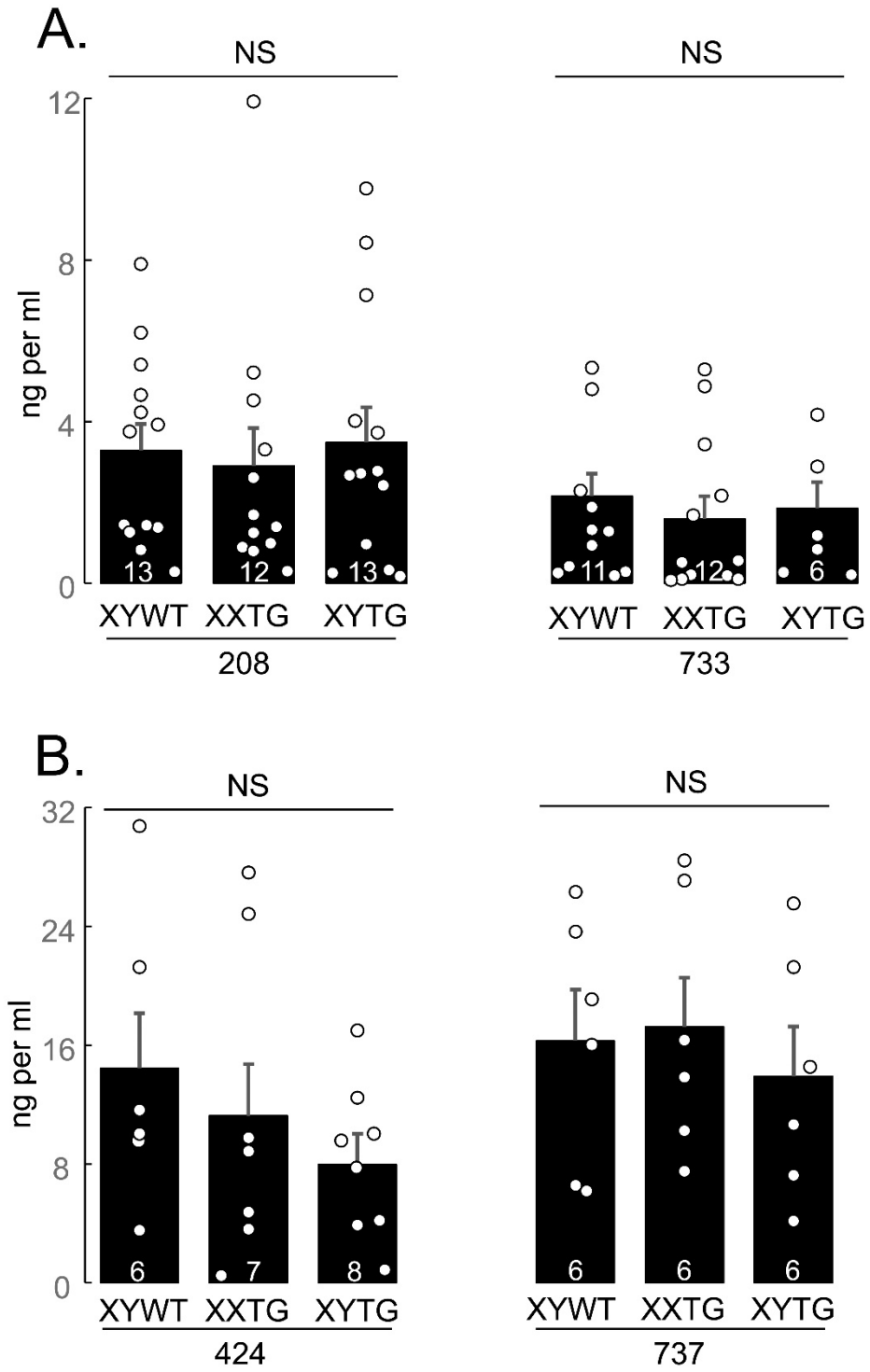

Figure 12. SNB morphology. Above, digital micrographs of thionin-stained transverse sections through the lumbar spinal cord of line 208, showing the medially located Spinal Nucleus of the Bulbocavernosus (SNB), with more neurons in groups with testes than in those with ovaries. Scale bar = 100 µm. Below, counts and soma areas of SNB motoneurons. Both motoneuron number and soma size varied significantly by genotype ($p<0.000001$), and all gonadal male groups were significantly different from all gonadal female groups (Tukey-Kramer, *** $p<0.001$). SNB number was lower in XYTG than XYWT (Tukey-Kramer, $p<0.05$). There was no significant variation between groups differing in sex chromosome complement.

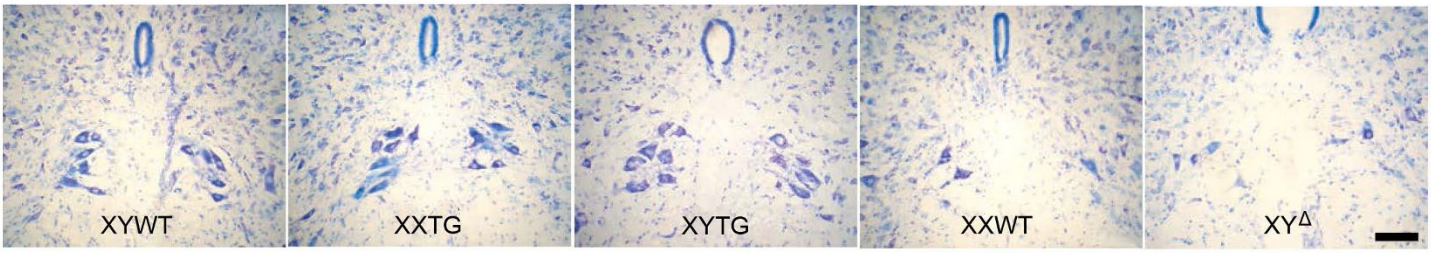

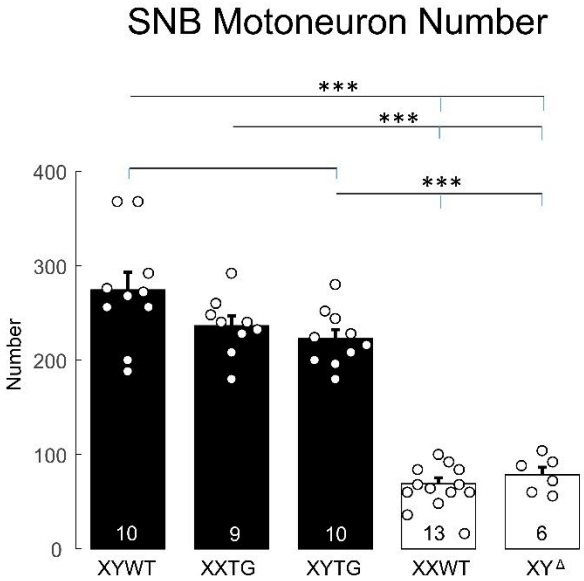

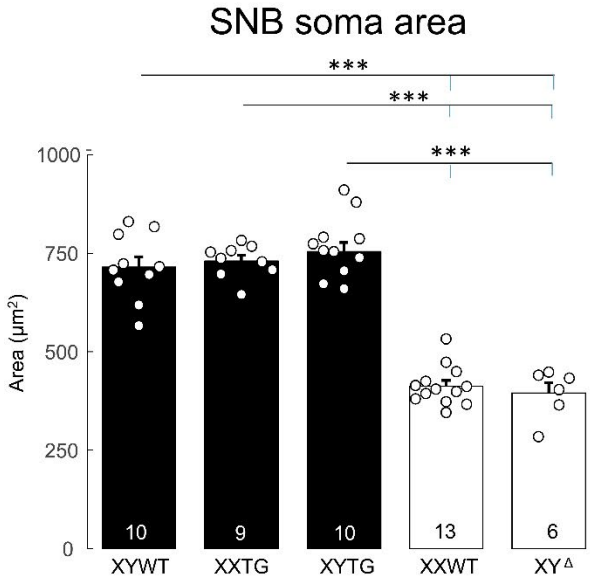

Figure 13. DLN morphology. Above, digital micrographs of thionin-stained transverse sections through the lumbar spinal cord show the laterally located Dorsolateral Nucleus (DLN) in line 208, showing more motoneurons in groups with testes than with ovaries. Also shown is the Retrodorsal Lateral Nucleus (RDLN), containing motoneurons that innervate an intrinsic muscle of the foot. Scale bar = 100 µm. Below, counts and soma areas of DLN motoneurons. The variation among groups was statistically significant (one-way ANOVA, $p<0.000001$ for DLN number, $p< 0.02$ for DLN area). All gonadal males groups differed significantly from all female groups for DLN number (Tukey-Kramer, *** $p<0.001$), but DLN soma area was not significantly different in in pairwise comparison of groups (Tukey-Kramer). For DLN soma area, a two-way ANOVA with factors of gonad type (ovaries vs. testes) and sex chromosome complement (XX vs. XY) revealed a main effect of gonad type ($p< 0.001$) but not sex chromosome complement.

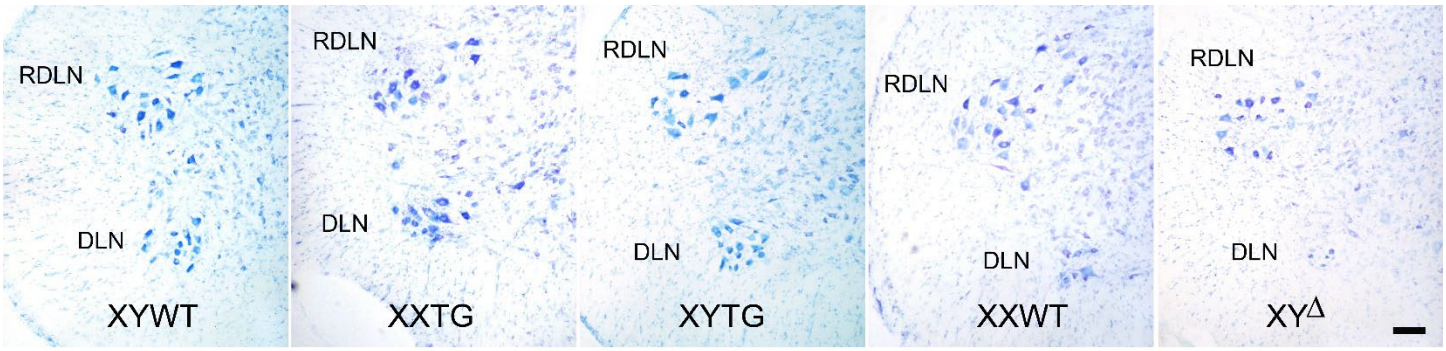

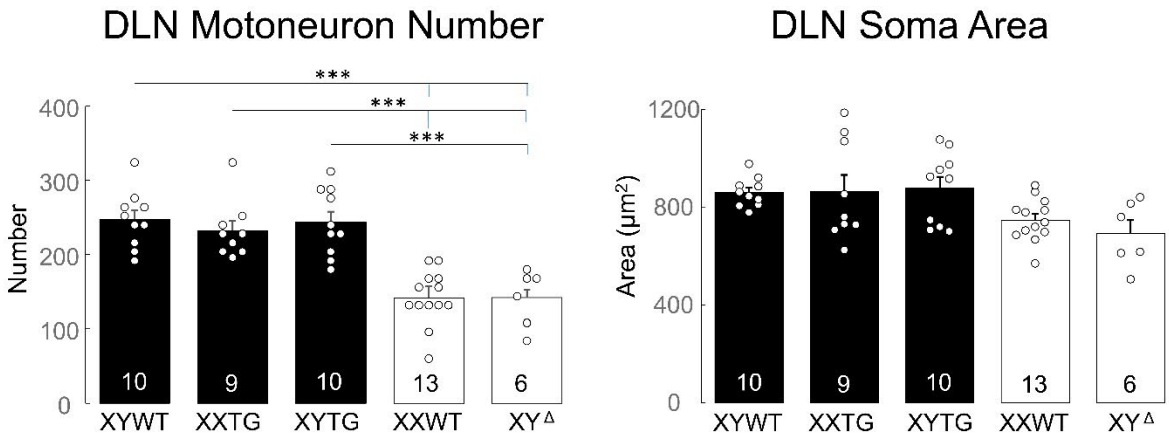

Figure 14. SDN-POA morphology. Above, digital micrographs of calbindin-immunoreactive cells in the Sexually Dimorphic Nucleus of the Preoptic Area of the hypothalamus (arrow) with nearby anterior commissure (AC) and third ventricle (3V) in line 208. The SDN-POA is larger in groups with testes than in those with ovaries. Scale bar = 300 µm. Below, measurements of SDN-POA volume, neuron number, and immunoreactive cell area. For each type of measurement, variation among groups was statistically significant (one-way ANOVA, $p < 0.000001$), and each group with testes was significantly different from each group with ovaries (Tukey-Kramer, *** $p < 0.001$). There was no significant variation between groups differing in sex chromosome complement.

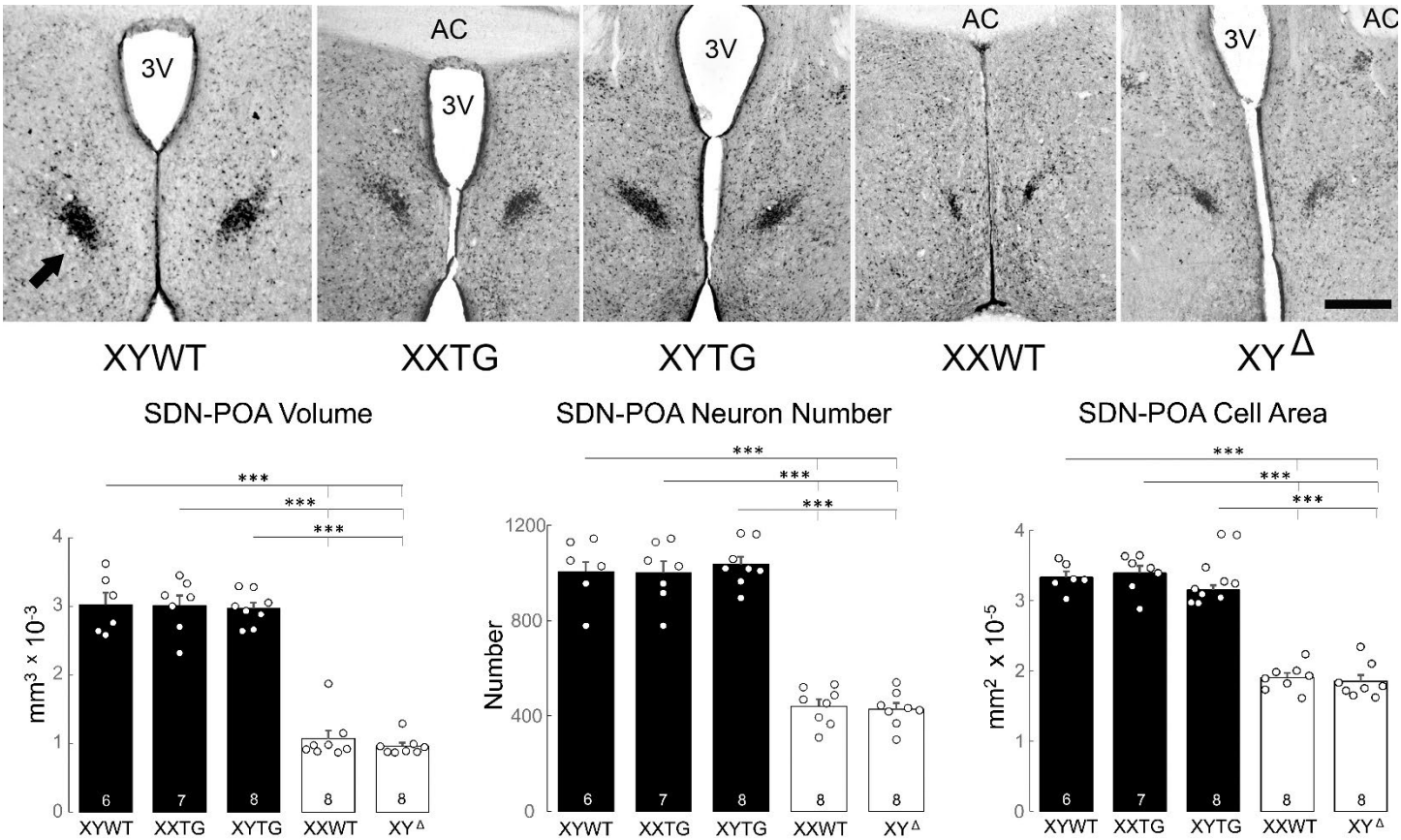
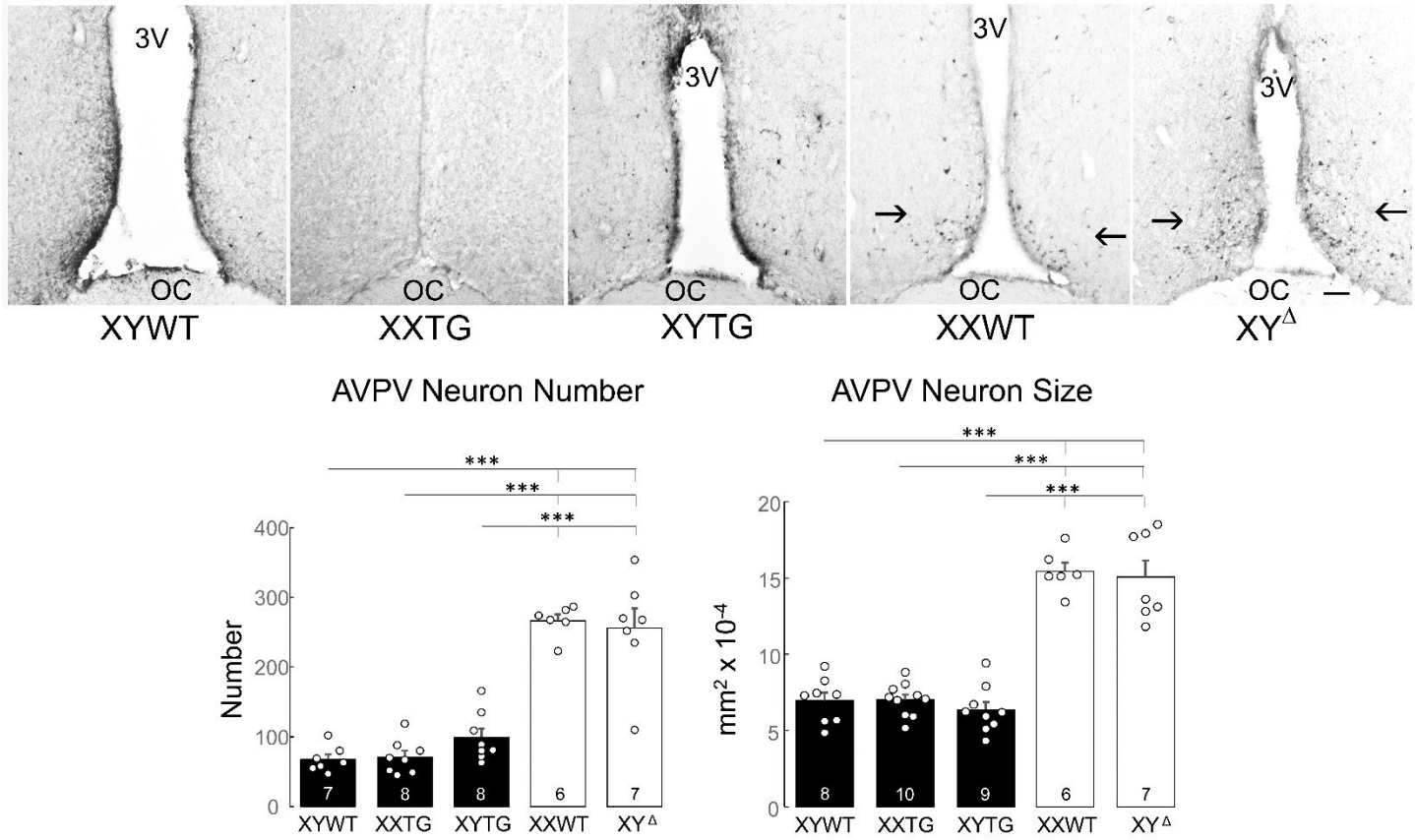
Figure 15. AVPV morphology. Above, digital micrographs of tyrosine-hydroxylase-immunoreactive neurons in the hypothalamic Anteroventral Periventricular Nucleus (AVPV) (arrows) adjacent to the third ventricle (3V) and above the optic chiasm (OC) in line 208 and progeny of XY^{Δ} females. Scale bar =100 µm. Many more TH-ir neurons are found in rats with ovaries than in rats with testes, independent of sex chromosome complement. Below, measures of numbers and size of TH-ir neurons. In both variables, variation among groups was significantly different (one-way ANOVA, $p < 0.000001$). Each gonadal male group had fewer neurons than each gonadal female group (Tukey-Kramer, *** $p < 0.001$). There was no apparent difference between groups differing in sex chromosome complement.